Evaluation of a Multivalent Artificial Opsonin to Target and Phagocytose Gram-Negative Bacteria

Henry Lee

A thesis

submitted in partial fulfillment of the

requirements for the degree of

Master of Science

University of Washington

2020

Committee:

James D. Bryers

Daniel M. Ratner

Program authorized to offer degree:

Bioengineering

University of Washington

Abstract

Evaluation of a Multivalent Artificial Opsonin to Target and Phagocytose Gram-Negative Bacteria

Henry Lee

Chair of the Supervisory Committee:
James D. Bryers
Department of Bioengineering

Hospital-acquired infections (HAIs) are a significant medical concern that must be tackled. HAIs cost the United States billions of dollars annually, and in 2002, were the sixth-leading cause of death [1-2]. *Klebsiella pneumoniae*, a gram-negative bacterial species, accounts for up to 10% of all HAIs [3-5]. Due to the prevalence of HAIs in the hospital environment, antibiotics have been traditionally used in an attempt to treat bacterial infections. Consequently, *Klebsiella pneumoniae* has developed resistance to a variety of antibiotics [3]. To compound the issue, this bacterial species can form biofilms to avoid opsonization and phagocytosis [6]. As a result, novel therapeutics that transcend antibiotics and antibodies must be developed.

One promising approach is to enhance the body's own immune system when fighting a bacterial infection. We have developed an artificial opsonin to recognize and phagocytose gram-negative bacteria. The artificial opsonin consists of three parts: (1) di-tuftsin, a peptide that activates and binds to the neuropilin-1 (Nrp1) receptor on macrophages to initiate an immune response, (2)

YI13WF, a peptide that has affinity to lipopolysaccharides (LPS) found on gram-negative bacterial membranes, and (3) a glycine linker to couple di-tuftsin and YI13WF together.

This thesis reports on the characterization of the artificial opsonin. First, the binding stoichiometry of the opsonin to several gram-negative and gram-positive bacteria was quantified. Second, the artificial opsonin's affinity to bind to RAW 264.7 mouse macrophages was evaluated. Finally, the efficacy of the opsonin to enhance RAW 264.7 macrophages' phagocytic capabilities of *Klebsiella pneumoniae* was determined.

Table of Contents

List of Figures

List of Tables

List of Abbreviations

5-FAM: 5-Carboxyfluorescein

Arg: Arginine

C: Cysteine

CD47: Cluster of differentiation 47

CD89: Cluster of differentiation 89

D-Ala-D-Ala: D-Alanyl-D-alanine

DMEM: Dulbecco's Modified Eagle Medium

DMSO: Dimethyl sulfoxide

EGFR: Epidermal growth factor receptor

EU/mL: Endotoxin units per milliliter

F: Phenylalanine

FITC: Fluorescein isothiocyanate

FcRs: Fc receptors

FcαRI: A specific type of FcR that recognizes IgA molecules

FcγR: A class of FcRs that recognize IgG molecules

FcγRIIa: A specific type of FcR that recognize IgG molecules

GFP: Green fluorescent protein

HAI: Hospital-acquired infection

HBSS: Hank's Buffered Saline Solution without calcium and magnesium

HI-FBS: Heat-inactivated fetal bovine serum

I: Isoleucine

IgA: Immunoglobulin A

IgG: Immunoglobulin G

IL6: Interleukin 6

K: Lysine

K_d: Dissociation constant

L: Leucine

LB: Lysogeny broth

LPS: Lipopolysaccharide

Lys: Lysine

M: Methionine

MIC: Minimum inhibitory concentration

MOI: Multiplicity of infection

Nrp1: Neuropilin-1

OD600: Optical density at 600 nm

PDGA: Poly-gamma-D-glutamic acid

PMNL: Polymorphonuclear leukocyte

PpIX: Protophophyrin IX

Pro: Proline

R: Arginine

SE Dymax: Super Enhanced Dmax Subtraction

TGFβ: Transforming growth factor beta

Thr: Threonine

TNF-α: Tumor necrosis factor-α

TSB: Tryptic soy broth

V: Valine

W: Tryptophan

Y: Tyrosine

YI12WF: An LPS-binding peptide with the sequence YVLWKRKRFIFI

YI13WF: An LPS-binding peptide with the sequence YVLWKRKRKFCFI

YW12: An LPS-binding peptide with the sequence YVLWKRKRMIFI

Acknowledgements

There are many people that I have to acknowledge because they all helped in some shape or form. Some helped me emotionally when I struggled and felt lost, some gave me insight on the problems I faced, and some did both.

I would like to thank my parents, Laurie and Kwok, and two older brothers, Andy and Eric, for being financially and emotionally supportive of me. While I may be far away from them, I can always count on them. They sculpted me into the individual I am today, and my successes trace back to them. They motivate me to work hard and finish strong. Hopefully, at the end of the day, I can give back to them for all the things they have done for me.

I would like to thank Professor Bryers and Associate Professor Ratner for being in my committee. We've had discussions about the expectations for graduation, and they have been involved in every step of the way. Besides that, I am thankful for Professor Bryers for giving me the opportunity to work in his lab. I learned much from the project, especially about what it takes to be a researcher. More importantly, I learned much about myself, whether it be how I view science, handle relationships, or tackle problems. Without the work that I did under Professor Bryers, I wouldn't have learned about the necessities to be a researcher and the principles that I value.

I would like to thank the current people in the Bryers group: Elizabeth Leber, Nathan Chan, Sarah Nick, and Thomas Hady. Thanks for providing a friendly atmosphere to work in. I have to give a big thanks to Elizabeth because she helped me adjust to the lab atmosphere and aided me when I first started on the project. She taught me how to do cell culture, bacteria culture, and so forth. In addition, as the lab manager, she kept the lab in order, which is no easy

task. Nathan Chan deserves credit for helping me understand what my first set of flow cytometry data meant and being a source of good conversations.

Alissa Bleem, a former member of the Bryers group, deserves significant recognition for all the mentorship that she gave me. As I progressed through the project. I had many questions, especially the fine details, about how the assays should be done. Luckily, Alissa answered all my questions in full, and I learned a lot from her. I could pick her brain about what I was doing, and our exchanges helped me thoroughly understand the significance of each step. If it wasn't for her, I would not have progressed as far as I had. As a result, I am grateful for the mentorship and support she provided.

I would like to thank Dylan Shea and Tatum Prosswimmer from the Dagget group for they were friendly faces that I saw every day. Dylan Shea was the peptides expert, and he answered all my questions about peptides. Thank you Dylan for all your help.

I would like to thank Xiaoping Wu, the manager of the Pathology Flow Cytometry Core Facility at UW. She helped set up the conditions (voltages, gates, etc.) of the LSRII flow cytometer I used. Furthermore, she gave me insight on how I should analyze my data. Without her, I wouldn't have any idea on how I should use the flow cytometer or know what to do with the data. Thank you for all your assistance Xiaoping.

I would like to thank Celine Diep for being my emotional anchor. Her unwavering support through the good times and bad helped me finish strong. She understood and empathized with my struggles, and I could always depend on her to give me a positive outlook even when the hardships seemed too difficult to overcome. I wouldn't be where I am at, in respect to personality and emotional state, without her, and I'm grateful for all that she has done.

I would like to thank the classmates and colleagues that I met at University of Washington. Ji Ho Kim has been a good friend and classmate throughout the two years. He helped me a lot in the two classes we had together, and he had meaningful insights on the struggles that I had with my project. He's been there for me for the past two years, and I appreciate his guidance and friendship. Joyce Lu and Yunshi Zhou have been my bioengineering friends for the past two years. We shared our struggles from the classes we took together. We also had some good conversations over the two years, and they helped me feel less of a stranger to the bioengineering department and UW as a whole. I'm grateful for their companionship.

I would like to thank the people that I played volleyball with, specifically Kevin Liao, Andrew Nguyen, Mark Liu, Kaylyn Lee, Norman Nguyen, and Natalie Au. Playing volleyball helped take my mind off research and enjoy my time at UW. Most importantly, I formed meaningful friendships with them that I hope continue once I graduate.

I would like to thank Victoria Thai, Dan Peng, John Kim, and Kevin Sibucao individuals from UC San Diego that I continue to talk to. Victoria is a close friend who has supported me throughout the three years I've known her, especially when I was struggling to adjust to UW. She's always a friend that I can talk to, and I can count on her to give me an unbiased opinion. Like Victoria, Dan is a close friend who I've known for the past three years. He has supported me, and I can look to him for help, whether it be about my project or life in general. He is someone that I can always go to whenever I have problems or want a second opinion. John Kim is my mentor and good friend who has always listened to my struggles about my project. He always lends an ear and gives me the unfiltered truth about how research works. Whenever I have issues with my project, I can always count on him to hear me out. Lastly, Kevin Sibucao is a good friend and my first mentor. He helped shape my view on what research is about, and he

gave me guidance about how to do future steps for my project from time to time. He sculpted my foundations as a researcher, and I thank him for that.

Lastly, I would like to thank individuals that are from my hometown, specifically Sonny Elizaldi, Adam Atamian, and Jo Gbujama. I've looked to Sonny for mentorship throughout the years because of his plethora of knowledge on a variety of topics. In addition, he helped me with the fundamentals of analyzing flow cytometry data. Adam and Jo are my close friends, and I can count on them for good times and conversations. Although we are all in different states, we have each other's backs.

It is obvious that I had much support from a variety of individuals. Each played a role in my life, and without them, I wouldn't be where I am today.

Dedication

I would like to dedicate my work to my parents, Laurie and Kwok, and older brothers, Andy and Eric. I wouldn't be where I am at today without them.

Chapter 1: Background

1.1 Significance

While people visit hospitals to get treated for a specific illness, they can potentially become sick for a different reason. In 2002, it was estimated that there were 1.7 million hospital-acquired infections (HAIs), and around 99,000 of those cases resulted in death [1-2]. As a result, hospital-acquired infections were the sixth leading cause of death in the United States. The estimated cost of these infections in the U.S. ranges from $5 billion to $10 billion annually [1]. Considering that the number of hospital-acquired infections has increased by 36% in the past 20 years, reducing the number of cases that occur is imperative [7].

Surgical-site infections, central-line-associated bloodstream infections, ventilator-associated pneumonia, and catheter-associated urinary tract infections account for approximately 75% of all hospital-acquired infections [7]. The traditional way to treat these infections is by using antibiotics. While the rate of antibiotic prescriptions did not change between 2006 and 2012, more powerful antibiotics were given to treat these infections instead [8]. By providing greater exposure to antibiotics, bacteria that were resistant to the drugs were naturally selected [9]. As a result, more than 70% of the bacteria that cause hospital-acquired infections are resistant to at least one of the drugs most commonly used to treat them [7].

1.2 Bacteria Pathology

Hospital-acquired infections are caused by an individual's own microflora, such as the bacterial flora on the patient's skin or in their respiratory tract, or microorganisms from other patients, health care workers, and visitors. A significant mechanism causing HAIs is the contamination of

materials, whether it be food, drugs, or medical equipment [10]. In respect to medical equipment, the implantation or insertion of a medical device can serve as a vehicle for opportunistic pathogens. For example, the insertion of catheters into the bladder can introduce bacteria into the urinary tract [10-11]. Another example is the implantation of prosthetic joints, where the prosthetic could be contaminated before implantation or become contaminated during surgery by airborne pathogens [12]. More than 30% of hospital-acquired infections are caused by gram-negative bacteria. They are the main agents in cases of urinary tract infections (45%) and ventilator-associated pneumonia (47%) [1].

Bacteria can adhere to surfaces through van der Waals and electrostatic forces. In addition, the surface's properties, such as hydrophilicity, porosity, and roughness, shape how well bacteria can adhere to the surface [13]. If the bacteria are allowed to colonize a surface, they will secrete an extracellular matrix comprised of polysaccharides, proteins, and nucleic acids; the collection of bacterial cells and extracellular matrix is called a "biofilm." The biofilm allows the bacteria to grow with minimal interruptions or threats because the matrix protects the bacteria from antibiotics and innate immune defenses, such as macrophages. Once the biofilm has matured, bacteria may disperse into the bloodstream due to shear stresses or quorum sensing signals that initiate community dispersal [14]. As a result, bacteria in the bloodstream can cause sepsis, which is identified by the onset of organ dysfunction away from the site of infection. Although already deadly, sepsis can evolve into a more severe form called septic shock, increasing the rate of mortality [15].

Although gram-negative bacteria cause only 30% of hospital-acquired infections, lipopolysaccharides (LPS), a key structural component in their membranes, are themselves clinical concerns [16]. LPS is an endoxin that has a significant role in causing sepsis and septic

shock syndromes. As LPS circulates in the bloodstream, phagocytic cells become activated and produce pro-inflammatory cytokines such tumor necrosis factor-α (TNF-α) and interleukin-6 (IL6). Although it is natural to produce proinflammatory cytokines in the presence of a bacterial infection, the overproduction of such cytokines may cause septic shock [17]. Thus, a treatment targeting gram-negative bacteria would help reduce the number and deaths caused by hospital-acquired infections.

1.3 *Klebsiella pneumoniae*

Klebsiella pneumoniae is a gram-negative opportunistic pathogen commonly found in the human mouth, intestines, and skin [1,18]. *K. pneumoniae* is responsible for 3 to 10% of hospital-acquired bacterial infections in first world nations [3-5]. A main source of transmission is person-to-person contact with a contaminated individual. Respiratory machines, catheters, or exposed wounds are other modes of transmission. *K. pneumoniae* is involved in pneumonia, wound infections, and sepsis [3, 19].

K. pneumoniae displays resistance to a variety of antibiotics: β-lactam, β-lactamase, and third and fourth generation cephalosporins [3]. Furthermore, *K. pneumoniae* can form biofilms, allowing the bacteria to avoid opsonization and phagocytosis [6]. Due to *K. pneumoniae*'s ability to form biofilms and resist antibiotics, infections by the bacteria tend to be chronic [18].

1.4 Immunology

1.4.1 Cellular response to Injury and Infection

In the presence of bacteria, tissue-resident macrophages become activated and release neutrophil chemoattractants to the site of infection. As the first line of defense, neutrophils release granules to destroy the pathogens and produce proteins that augment monocyte recruitment. Monocytes

that have arrived at the infection site differentiate into M1 macrophages that can phagocytose and degrade the pathogens. Pathogens undergo phagocytosis when they are either opsonized by antibodies or complement proteins or when pathogen recognition structures on the bacteria are directly recognized by macrophages [20-21].

1.4.2 Opsonin Dependent Phagocytosis

While macrophages can recognize microorganisms that have not been opsonized by antibodies or complement factors, opsonization labels foreign pathogens to make them more readily phagocytosed and destroyed by phagocytic cells [22-24]. Opsonins, in the form of complement proteins or antibodies, are recognized by complement receptors and Fc receptors (FcRs) on immune cells, respectively [24-25]. Besides opsonins, other factors may induce phagocytosis such as the peptide tuftsin [23]. Tuftsin will be discussed in depth in section 1.7. In this section, opsonin dependent phagocytosis utilizing FcRs will be examined.

Macrophages express varying degrees of inhibitory and activating FcRs on their membranes. Phagocytosis is initiated when the sum of activating and inhibiting signals reach a certain threshold. When an invading particle or pathogen is opsonized with immunoglobulin G (IgG), the Fc portion of the IgG is recognized by Fc receptors specific to IgG (FcγR) on the phagocytic cell. Then, the Fc portion of the IgG binds to FcγR to initiate phagocytosis. FcγRIIa, a specific type of FcγR, will aggregate to make multiple binding contacts with the opsonized particle. The aggregation induces integrin activation, which allows even more FcγRs to interact with the particle. These binding interactions signal to the macrophages that an invading particle is present. As a result, the cell's actin cytoskeleton remodels itself so that the cell membrane can undergo changes. Specifically, actin remodeling leads to the formation of the pseudopodia. Nucleation of actin filaments extends the pseudopodia to surround the particle and internalize it

with a structure called a phagosome. Afterwards, the phagosome is sealed as the actin filaments are depolymerized. Eventually, the phagosome will mature into a phagolysosome in order to eliminate the ingested particle [26].

1.5 LPS Recognition Peptide YI13WF

Liu et al. [27] used a lipopolysaccharide (LPS) binding antimicrobial peptide YI13WF (YVLWKRKRKFCFI-Amide) conjugated to protophophyrin IX (PpIX) to fluorescently image and photodynamically inactivate drug-resistant gram-negative bacterial strains. In order to determine YI13WF's affinity to bacteria, the authors compared the fluorescence intensity between PpIX-YI13WF and PpIX stained cells. They found that PpIX-YI13WF stained gram-negative bacteria showed 8 times greater fluorescence than PpIX stained gram-negative bacteria. In addition, minimum inhibitory concentrations (MICs) for four gram-negative bacterial species were lower when the bacteria were exposed to YI13WF as opposed to PpIX. These two findings indicate that YI13WF showed specificity to the LPS present on gram-negative bacterial membranes [27].

YI13WF is an analogue of series of peptides YW12 (YVLWKRKRMIFI) and YI12WF (YVLWKRKRFIFI). YW12, the original LPS-binding peptide, was designed by studying the amino acid residues of cocrystal structure of FhuA, a β-barrel outer membrane protein of *E. coli*, and LPS. From their examination, the authors determined what residues would be needed to bind to the cocrystal structure [28]. YI12WF was expected to improve upon YW12 by enhancing interactions with LPS. Bhunia et al. [17] determined that YI12WF could bind to LPS and neutralize it. More specifically, 100 nM of YI12WF could inhibit 95% of LPS at LPS concentrations of 1 and 3 endotoxins/mL (EU/mL). They proposed that positive charge residues

KRKR interact with the polar regions and phosphate heads of LPS. Furthermore, they believed that W and F located at the 4^{th} and 9^{th} position of the peptide, respectively, secured KRKR's insertion in LPS by binding to the hydrophobic tails of LPS [17].

In the same publication, Bhunia et al. [17] determined the minimum inhibitory concentrations for two gram-negative bacteria strains (*E. coli* and *P. aeruginosa* ATCC27853) and two gram-positive bacteria strains (*S. aureus* ATCC25923 and *B. subtilis*) when incubated with a variety of antimicrobial peptide candidates. For YI12WF, the MICs across all strains were similar if not the same, ranging between 10 and 30 μM. The authors did not explain why the peptide could be inhibiting gram-positive bacteria at a similar rate as gram-negative bacteria [17].

1.6 Macrophage Recognition Peptide Tuftsin

Tuftsin is a tetrapeptide (Thr-Lys-Pro-Arg) that stimulates phagocytic cell function. The sequence is residues 289 to 292 of the heavy chain of leukokinin's Fc region, and it is formed from the cleavage of a specific immunoglobulin G (IgG) called leukokinin [29-31]. Activation of phagocytic cells with tuftsin or polytuftsin, which consists of several consecutive repeats of tuftsin, augments phagocytosis, motility, immunogenic stimulation, the number of antibody-forming cells, bactericidal activity, and tumoricidal activity [29]. A peptide containing two tuftsin repeats (di-tuftsin) increased affinity to tuftsin receptors on rabbit peritoneal polymorphonuclear leukocytes (PMNLs) and antitumor capabilities in mice. However, stimulation of phagocytosis between di-tuftsin and tuftsin were similar [32]. Nonetheless, tuftsin or tuftsin-like peptides have been produced and have shown promise in treating bacterial

infections [33], fibrosarcoma [34], and epidermal growth factor receptor (EGFR)- and cluster of differentiation 47 (CD47)-overexpressing cancers [35].

Tuftsin activation occurs when it binds and forms clusters to plasma membrane receptors that are found on PMNLs, monocytes, macrophages, and granulocytes. Afterwards, tuftsin is internalized by the phagocytic cells. The rate of receptor-peptide cluster formation and internalization is dependent on temperature and concentration of tuftsin present. Larger concentrations of tuftsin increased the rates compared to lower concentrations. Furthermore, the timeline of events occurred faster at 37°C than 22°C, and no interactions between cells and tuftsin were observed at 4°C [32, 36].

Since tuftsin originates from the Fc region of the IgG leukokinin, it was postulated that the tuftsin receptor was the same or similar to the Fc receptor. Previous studies had shown that Fc peptidic fragments could bind to the tuftsin receptor. However, it was ultimately determined that the Fc receptor was not the same as the tuftsin receptor, but the two shared similarities that could possibly indicate that the tuftsin receptor derived from the Fc receptor [32]. After those findings in the 1980s, little had been done to determine an exact tuftsin receptor and tuftsin signaling pathway until recently. Von Wronski et al. [37] identified neuropilin-1 (Nrp1) as a tuftsin receptor. Nissen et al. [38] discovered that once tuftsin binds to Nrp1, the transforming growth factor beta (TGFβ) signaling pathway is followed to induce tuftsin's effects on phagocytic cells.

1.7 Strategies for Enhancement of Phagocytosis

1.7.1 Previous Approaches

Researchers have previously produced bispecific recognition molecules that target both the pathogen and a phagocytosing cell. In doing so, the pathogen and the phagocytosing cell should come in close proximity of one another in order to augment phagocytosis. The Taylor group created opsonins specific to *Escherichia coli* [39], *Pseudomonas aeruginosa* [40], and *Staphylococcus aureus* [41]. Each opsonin consisted of a monoclonal antibody specific to complement receptor 1 of primate erythrocytes and a monoclonal antibody specific to the pathogen. All three different opsonins were shown to increase the phagocytosis and killing of the targeted pathogen [39-41].

Kobayashi et al. [42] created an artificial opsonin targeting *Porphyromonas gingivalis* by linking a monoclonal antibody specific to the hemagglutinin domain of *P. gingivalis* to a monoclonal antibody specific to the polymorphonuclear leukocyte FcαRI (CD89) receptor. FcαRI (CD89) receptor is a specific type of FcR that recognizes immunoglobulin A (IgA) molecules. *P. gingivalis* opsonized with this bispecific molecule were more susceptible to be phagocytosed and killed by PMNLs than bacteria opsonized with a monoclonal antibody specific to the hemagglutinin domain [42].

Tacken et al. [43] was able to target *E. coli*, *Candida albicans*, and influenza A by developing a bispecific antibody utilizing a monoclonal antibody fragment against surfactant protein D, a collectin that has an affinity for carbohydrates on many pathogens, and a monoclonal antibody fragment directed towards human FcαRI (CD89). The chimeric protein was

able to increase the uptake of *E. coli*, *Candida albicans*, and influenza A and the killing of *E. coli* and *Candida albicans* by human neutrophils [43].

Bruno et al. [44] generated an artificial opsonin targeting *Bacillus anthracis*. DNA aptamers specific to poly-gamma-D-glutamic acid (PDGA), a major structural component of *B. anthracis* capsules, were linked to an Fc fragment of murine IgG. They tested their molecule against magnetic beads coated with PDGA to avoid working with the virulent strain. Their preliminary work determined that opsonization of the beads with their bispecific recognition molecule increased phagocytosis by murine macrophages up to three-fold [44].

While these designs have shown success, they had one of possibly two limitations: (1) they targeted specific pathogens due to the usage of monoclonal antibodies or DNA aptamers or (2) they targeted surface receptors of the phagocytosing cells that made the pathogen and the phagocytosing cell come in close proximity of one another but not necessarily activate phagocytosis [45-46].

Katzenmeyer and Bryers [45, 47] resolved these issues by coupling vancomycin, an antibiotic that recognizes the terminal D-Alanyl-D-alanine (D-Ala-D-Ala) in gram-positive bacterial membranes, to the Fc portion of an IgG to activate phagocytic cells. They showed that vancomycin was able to bind to several gram-positive bacterial species. Most importantly, they showed that their construct increased phagocytosis of gram-positive bacteria in comparison to no treatment or treatment with the Fc portion of IgG. Thus, this artificial opsonin could be used to target multiple gram-positive bacterial species for phagocytosis [45, 47].

1.7.2 Multivalent Artificial Opsonin to Target and Phagocytose Gram-negative Bacteria

Following in the footsteps of Katzenmeyer, we have developed a multivalent artificial opsonin to enhance the recognition and phagocytosis of gram-negative bacteria by murine macrophages. The sequence of the opsonin is **TKPRTKPR**GGGG**YVLWKRKRKFCFI**, and it consists of di-tuftsin, a glycine linker, and YI13WF. YI13WF recognizes the LPS in gram-negative bacteria, and di-tuftsin augments phagocytosis in phagocytic cells. The following chapters detail the artificial opsonin's binding affinity to gram-negative bacteria, gram-positive bacteria, and murine macrophages and efficacy to enhance phagocytosis.

Chapter 2: Binding of 5-FAM Labeled Artificial Opsonin to Gram-negative and Gram-positive bacteria

2.1 Abstract

In this chapter, the degree to which the artificial opsonin binds to gram-negative and gram-positive bacteria is examined. 1 mL of 9.3 x 10^7 cells/mL of gram-negative bacteria *Klebsiella pneumoniae* and *Pseudomonas aeruginosa* PAO1 and gram-positive bacteria *Enterococcus faecalis* and *Staphylococcus epidermidis* RP62A were incubated with a fluorescently labeled version of the artificial opsonin. Flow cytometry was used to assess the extent to which the bacteria were opsonized. The amount of opsonin bound per bacteria increased in a hyperbolic saturation kinetics fashion. The minimum opsonin concentration to reach greater than 98.5% of opsonin-bound cells for *K. pneumoniae*, *S. epidermidis* RP62A, *E. faecalis*, and *P. aeruginosa* PAO1 were 3 µM, 2 µM, 1 µM, and 10 µM, respectively. Thus, the artificial opsonin shows promise to bind to all bacterial strains, expanding the breadth of the artificial opsonin's purpose.

2.2 Introduction

The extent to which varying concentrations of 5-FAM labeled artificial opsonin binds to gram-negative and gram-positive bacteria was examined. Determining the binding curves between artificial opsonin and varying bacterial species addresses how much opsonin is needed to saturate a specific amount of bacteria. Greater opsonization of the bacteria will potentially maximize phagocytosis.

The FlowJo Population Comparison functions Overton cumulative histogram subtraction and Super-Enhanced Dmax Subtraction (SE Dymax) are algorithms used in flow cytometry data

interpretation to generate dose-response curves. They help determine the percentage of fluorescent cells with bound peptide or protein that are found in a sample compared to the control. The population comparison functions are more suitable for creating dose-response curves because it considers the possibility that there are positive cells (cells with bound peptide or protein) in the fluorescence overlap between controls and samples. In a traditional gating scheme where the user forms gates, the overlap would have zero positive cells since the overlap falls under the range of control fluorescence. However, binding is never a black and white situation; there is a range of positive cells where some cells have more material bound to it than others. Thus, these two algorithms are more suited to generate a dose-response curve than a traditional gating scheme [48].

Although these two algorithms fall under the same category, the SE Dymax method is better suited than the Overton method. The Overton method essentially subtracts the sample's histogram from the control histogram [49]. The difference between the sample and control histograms determines the percentage of positive cells. Unlike Overton, SE Dymax includes normalization and population estimations to perform better histogram subtractions. The normalization makes the histograms used for subtraction the same shape, which is useful if the control and sample histograms have varying amounts of data points. The population estimation predicts the probability distribution function of the positive population, helping to create a better fit to noisy data. Thus, SE Dymax is preferred over the Overton method because it helps create a more accurate subtraction of the histograms [48]. As a result, SE Dymax was utilized to determine the degree to which artificial opsonin bound to a specific concentration of bacteria.

2.3 Materials and Methods

2.3.1 Preparation of the Bacteria Culture

Klebsiella pneumoniae, Pseudomonas aeruginosa PAO1, *Enterococcus faecalis,* and *Staphylococcus epidermidis* RP62A were the four bacteria species used. More information about each can be found in Table 2.3.1.1. *K. pneumoniae*, *P. aeruginosa* PAO1, and *E. faecalis* were grown in 10 mL of Lysogeny broth (LB) Miller medium (Fisher BioReagents) for 16 hours at 37°C and 180 rpm in a New Brunswick Scientific Excella E24 incubator shaker. *S. epidermidis* RP62A was grown in 10 mL of Tryptic Soy Broth (TSB) medium (Becton Dickenson) for 16 hours at 37°C and 180 rpm in a New Brunswick Scientific Excella E24 incubator shaker.

After 16 hours, different amounts of bacteria for each species were aliquoted out and washed twice. For all bacterial species, standard curves relating concentration of cells/mL to optical density at 600 nm (OD600) were used to determine the volume of bacterial culture needed to reach a specific amount of bacteria. For *K. pneumoniae* and *P. aeruginosa* PAO1, 1 mL of 9.3×10^7 cells/mL were aliquoted out into 1.5 mL centrifuge tubes. The bacterial suspensions were centrifuged at 10,000 rcf for 6 minutes with an Eppendorf 5417c centrifuge. The supernatants were removed, and the bacterial pellets were resuspended in 1 mL of Hank's buffered saline solution without calcium and magnesium (HBSS, Sigma-Aldrich). The centrifugation and supernatant extraction steps were repeated once. The bacteria was then resuspended in 950 µL of HBSS with 5% heat-inactivated fetal bovine serum (HI-FBS, Gibco) at a concentration of 9.8×10^7 cells/mL. The steps described for the preparation of *K. pneumoniae* and *P. aeruginosa* PAO1 bacteria is illustrated in Figure 2.3.1.1.

For *E. faecalis,* 1 mL of 1.9×10^8 cells/mL was aliquoted out into 1.5 mL centrifuge tubes. The bacterial suspensions were centrifuged at 10,000 rcf for 6 minutes with an Eppendorf

5417c centrifuge. The supernatants were removed, and the bacterial pellets were resuspended in 1 mL of HBSS. The centrifugation and supernatant extraction steps were repeated once. The bacteria were then resuspended in 1 mL of HBSS with 5% HI-FBS at a concentration of 1.9 x 10^8 cells/mL. A 1:2 dilution was performed, where 500 µL was taken out of the centrifuge tubes and disposed. Afterwards, 450 µL of HBSS with 5% HI-FBS was added to the tubes with bacteria to be opsonized. Thus, there was 950 µL of bacteria and HBSS with 5% HI-FBS at a concentration of 9.8 x 10^7 cells/mL. The steps described for the preparation of *E. facecalis* bacteria is illustrated in Figure 2.3.1.1.

For *S. epidermidis* RP62A, 1 mL of 9.3 x 10^8 cells/mL was aliquoted out into 1.5 mL centrifuge tubes. The bacterial suspensions were centrifuged at 10,000 rcf for 6 minutes with an Eppendorf 5417c centrifuge. The supernatants were removed, and the bacteria were resuspended in 1 mL of HBSS. The centrifugation and supernatant extraction steps were repeated once. The bacterial pellets were then resuspended in 1 mL of HBSS with 5% HI-FBS at a concentration of 9.3 x 10^8 cells/mL. A 1:10 dilution was performed, where 900 µL was taken out of the centrifuge tubes and disposed. Afterwards, 850 µL of HBSS with 5% HI-FBS was added to the tubes with bacteria to be opsonized. Thus, there was 950 µL of bacteria and HBSS with 5% HI-FBS at a concentration of 9.8 cells/mL x 10^7. The steps described for the preparation *S. epidermidis* RP62A bacteria is illustrated in Figure 2.3.1.1.

2.3.2 Opsonization of the Bacteria

0.2 mg of lyophilized 5-FAM labeled artificial opsonin (GenScript) were diluted in 40 uL of ultrapure water. Stock solutions of 10 µM, 20 µM, 40 µM, 60 µM, 80 µM, 100 µM, and 200 µM were made from the base opsonin solution. Then, 50 µL of a stock solution was pipetted into 1.5 mL tubes with 950 µL of bacteria at concentrations of 9.8 cells/mL x 10^7. As a result, labeled

opsonin concentrations of 500 nM, 1 µM, 2 µM, 3 µM, 4 µM, 5 µM, and 10 µM were used for 1 mL of 9.3 x 10^7 cells/mL of *K. pneumoniae* and *P. aeruginosa* PAO. Labeled opsonin concentrations of 500 nM, 1 µM, 2 µM, 3 µM, and 10 µM were used for 1 mL of 9.3 x 10^7 cells/mL of *E. faecalis* and *S. epidermidis* RP62A. For the controls, 50 µL of ultrapure water was added. Tubes were end-over-end mixed in the dark at 37°C for one hour.

After one hour, all samples were put on ice for 5 minutes. Using an Eppendorf 5417c centrifuge, the tubes' contents were centrifuged at 10,000 rcf for 6 minutes at 4°C. The supernatant was removed, and the bacteria were resuspended in 1 mL in chilled HBSS. The centrifugation and supernatant extraction steps were repeated once. Afterwards, the bacterial pellets were resuspended in 1 mL of chilled HBSS with 1% HI-FBS. Figure 2.3.2.1 describes the steps that were taken to opsonize the bacteria.

2.3.3 Flow Cytometry

Depending on which bacteria species, dilutions were made in 5 mL flow cytometry tubes so that the bacteria could be easily detected on the flow cytometer. *K. pneumoniae* and *P. aeruginosa* PAO1 were diluted 1:50, *S. epidermidis* RP62A was diluted 1:5, and *E. faecalis* was diluted 1:2. Figure 2.3.2.1 reiterates the dilutions necessary for each bacteria species.

The flow cytometry tubes were placed on ice. All the samples analyzed on a BD Biosciences LSRII flow cytometer. One color flow cytometry was utilized because the opsonin was the only fluorescent component that needed to be recorded. The amount of fluorescence recorded correlated to the percentage of cells that had bound to the opsonin. The bacterial suspensions were delivered to the flow cytometer. The threshold rate, the number of events detected per second, was adjusted so that the number of events associated with the bacterial suspensions well surpassed the number of events associated with a HBSS with 1% HI-FBS

solution. 10,000 events without any gates were collected. All the voltages were kept the same from experiment to experiment and across all bacterial species to ensure that all experiments, and all bacterial species, could be compared with one another.

2.3.4 Data Analysis

FlowJo software version 10.1 (Treestar) was used for data analysis. The events collected were gated on side scatter area versus forward scatter area and forward scatter width versus forward scatter area. The gated samples' 5-FAM fluorescence histograms were used to determine the degree to which the opsonin bound to the bacteria. With the SE Dymax algorithm in the FlowJo software, individual experimental samples were compared to all the individual control samples that were used throughout the experiments for a given bacterial species. The average of all the sample SE Dymax values for a certain opsonin concentration was used to provide an overall assessment of the percentage of the bacteria-opsonin complex present at a given applied opsonin concentration.

From the average percentage of fluorescence of each bacterial species at a specific opsonin concentration, the number of bacteria in each sample, and Avogadro's number, the number of opsonins bound to one bacterial cell of each bacterial species was determined. The concentration of applied artificial opsonin was converted into moles, and the moles was converted into number of molecules by using Avogadro's number. Based on the average percentage of fluorescence of each bacterial species at a specific opsonin concentration and the number of bacteria in each sample, the number of bacteria that were fluorescent for a given opsonic concentration was calculated. Afterwards, the number of opsonin molecules bound to one bacterial cell of each bacterial species was determined.

2.4 Results

Based on the histograms of all the samples across all bacterial species, augmenting the applied opsonin concentration correlated to an increase in bacterial 5-FAM fluorescence. However, the appearance of the bacterial species' histograms differed. Gram-negative bacteria *K. pneumoniae* and *P. aeruginosa* PAO1 exhibited single-peak curves that shifted towards higher values of 5-FAM fluorescence with increasing concentration of applied opsonin. On the other hand, gram-positive bacteria *E. facealis* and *S. epidermidis* RP62A exhibited two-peak curves that shifted towards higher values of 5-FAM fluorescence with increasing concentrations of applied opsonin. This was rather unexpected in that this opsonin was designed to recognize only gram-negative bacteria, and these results will be discussed in 2.5.2. Figures 2.4.1, 2.4.3, 2.4.5, and 2.4.7 show the histograms obtained from FlowJo for *K. pneumoniae, P. aeruginosa* PAO1, *S. epidermidis* RP62A, and *E. faecalis*, respectively.

According to the values obtained from SE Dymax, the minimum opsonin concentration to reach greater than 98.5% of fluorescent cells with bound opsonin (based on a sample size of n = 4) for *K. pneumoniae, S. epidermidis* RP62A, *E. faecalis*, and *P. aeruginosa* PAO1 were 3 μM, 2 μM, 1 μM, and 10 μM, respectively. A plot of the percentage of fluorescent cells versus opsonin concentration can be seen in Figures 2.4.2, 2.4.4, 2.4.6, and 2.4.8 for *K. pneumoniae, P. aeruginosa PAO1, S. epidermidis* RP62A, and *E. faecalis*, respectively.

The number of artificial opsonin molecules bound to a bacterial cell for *K. pneumoniae*, *P. aeruginosa* PAO1, *S. epidermidis* RP62A, and *E. faecalis* were $2.48 * 10^7$ molecules/cell, $2.61 * 10^7$ molecules/cell, $2.16 *10^7$ molecules/cell, and $1.05*10^7$ bacteria/cell, respectively.

2.5 Discussion

2.5.1 Gating method for Bacteria

Gates made for bacteria are not as stringent as ones made for larger cells such as RAW 264.7 macrophages. Bacteria are too small to be differentiated from the blank solution (HBSS with 1% HI-FBS), allowing the particles inherent in the blank solution to be considered as viable data points. In order to avoid this issue, the events captured for the sample must be magnitudes larger than the events captured for the blank. In doing so, the impact from the blank on the data is minimized. For these experiments, 0 to 20 events were captured per second for the blank, while 200 to 300 events per second were captured for the samples. Furthermore, with a high opsonin concentration, the blank's effect would become negligible. The opsonin would saturate the bacteria to the point that data coming from the blank solution would not affect the overall generation of the dose-response curve.

2.5.2 Binding of Opsonin to Gram-negative and Gram-positive bacteria

Ideally, the 5-FAM fluorescence histograms would have one peak, and the variety of fluorescent cells with bound opsonin would be within that one peak. The gram-negative bacteria follow this trend, but the gram-positive bacteria do not. Theoretically, there should not be any binding with gram-positive bacteria since the opsonin was designed to be specific to gram-negative bacteria. However, it is possible that the artificial opsonin's di-tuftsin component, or even YI13WF, could be non-specifically binding to gram-positive bacteria. The two peaks in the 5-FAM fluorescence histograms seen in gram-positive bacteria when incubated with high concentrations of opsonin may originate from the fact that there are two distinct populations of fluorescent cells with bound opsonin. One population would be associated with less opsonin binding, while the other would be affiliated with greater opsonin binding. Hypothetically, as the opsonin concentration

increases, a shift towards the peak with the higher fluorescence range would occur. This phenomena is evident in Figures 2.4.5 and 2.4.7 because the right peak increases in size at the expense of the left peak. Nevertheless, it is somewhat unexpected to see the opsonin binding to both gram-negative and gram-positive bacteria. However, this result is plausible because it was foreshadowed by Bhunia et al. [17] since gram-positive bacteria had similar MICs as gram-negative bacteria when incubated with YI12WF. Their findings indicate that the LPS recognition peptide may non-specifically bind to gram-positive bacteria.

In order to determine whether YI13WF or di-tuftsin of the artificial opsonin is binding to gram-positive bacteria, binding assays of the individual components would be performed. Fluorescently labeled YI13WF and di-tuftsin would undergo the same binding study performed for the artificial opsonin. The analysis of their outputted 5-FAM fluorescence histograms would indicate what segment is binding to gram-positive bacteria.

2.6 Conclusion

The opsonin bacterial binding assays illustrated that the artificial opsonin has exhibited binding affinity to both gram-negative and gram-positive bacteria. In addition, increasing the amount of applied opsonin appeared to saturate the bacteria at a concentration of 9.3×10^7 cells/mL. These results indicate that the artificial opsonin can completely opsonize bacteria, provided that the concentration is high enough. Furthermore, it shows that the artificial opsonin's function may be more multi-faceted than was expected. Bhunia et al. [17] showed this possibility since YI12WF acted as an antimicrobial peptide to both gram-positive and gram-negative bacteria.

For the phagocytosis assay with RAW 264.7 cells, described in Chapter 4, only *K. pneumoniae* was used.

Table 2.3.1.1: Description of the four bacterial species used in determining the degree to which the 5-FAM labeled opsonin binds to gram-negative and gram-positive strains. The descriptions in the "Type" and "Source" category are generic because either the laboratory database or ATCC does not any specific information on the bacteria strain.

Strain	**Gram-negative or gram-positive?**	**Type**	**Source**
Staphylococcus epidermidis RP62A	Gram-positive	Laboratory	Clinical strain
Enterococcus faecalis	Gram-positive	Laboratory	ATCC 49332
Klebsiella pneumoniae	Gram-negative	Blood, United States	ATCC BAA-2789
Pseudomonas aeruginosa PAO1	Gram-negative	Laboratory	Clinical strain

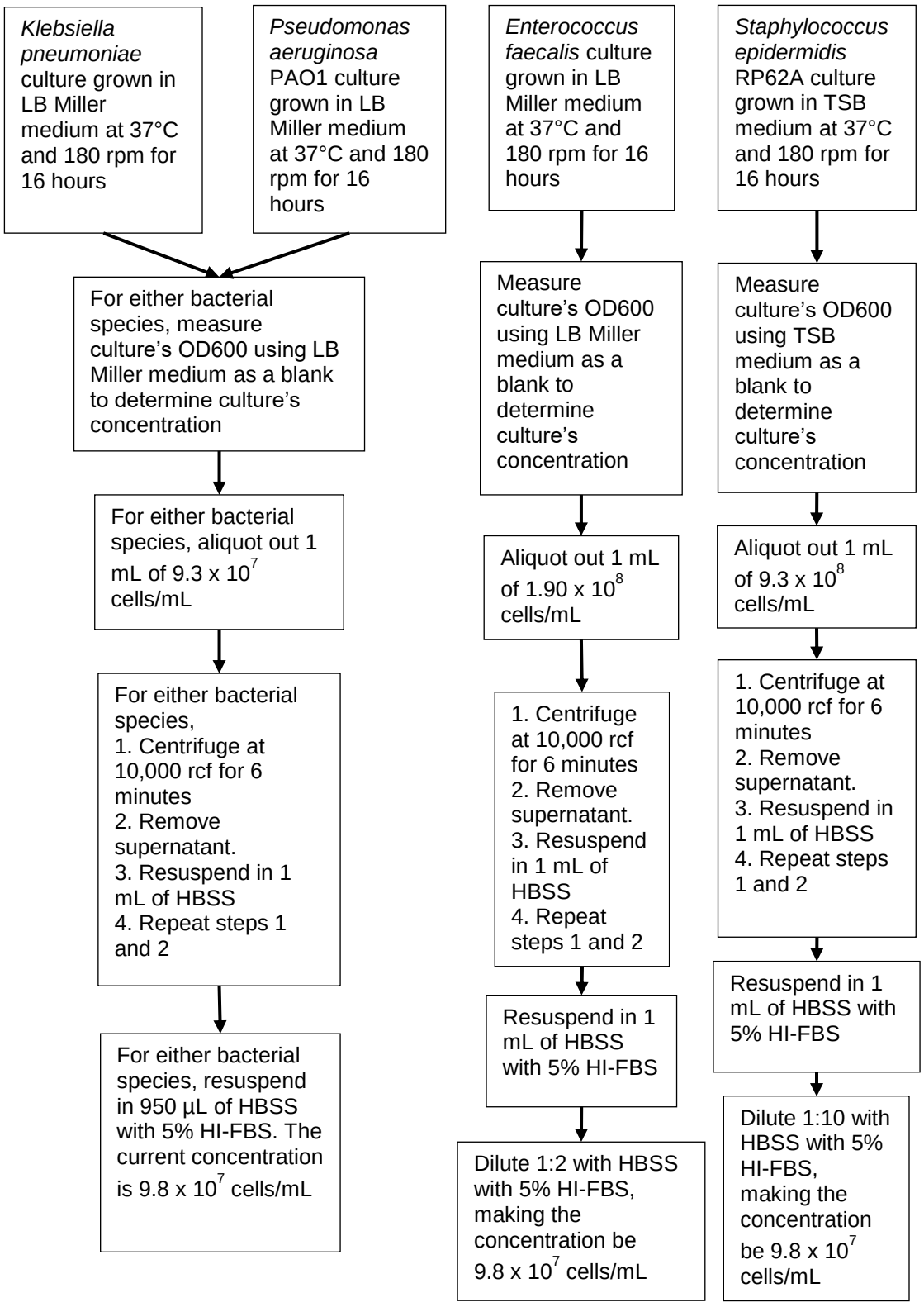

Figure 2.3.1.1: A flowchart describing how the bacteria cultures of the four bacterial species were prepared for the opsonin binding assay

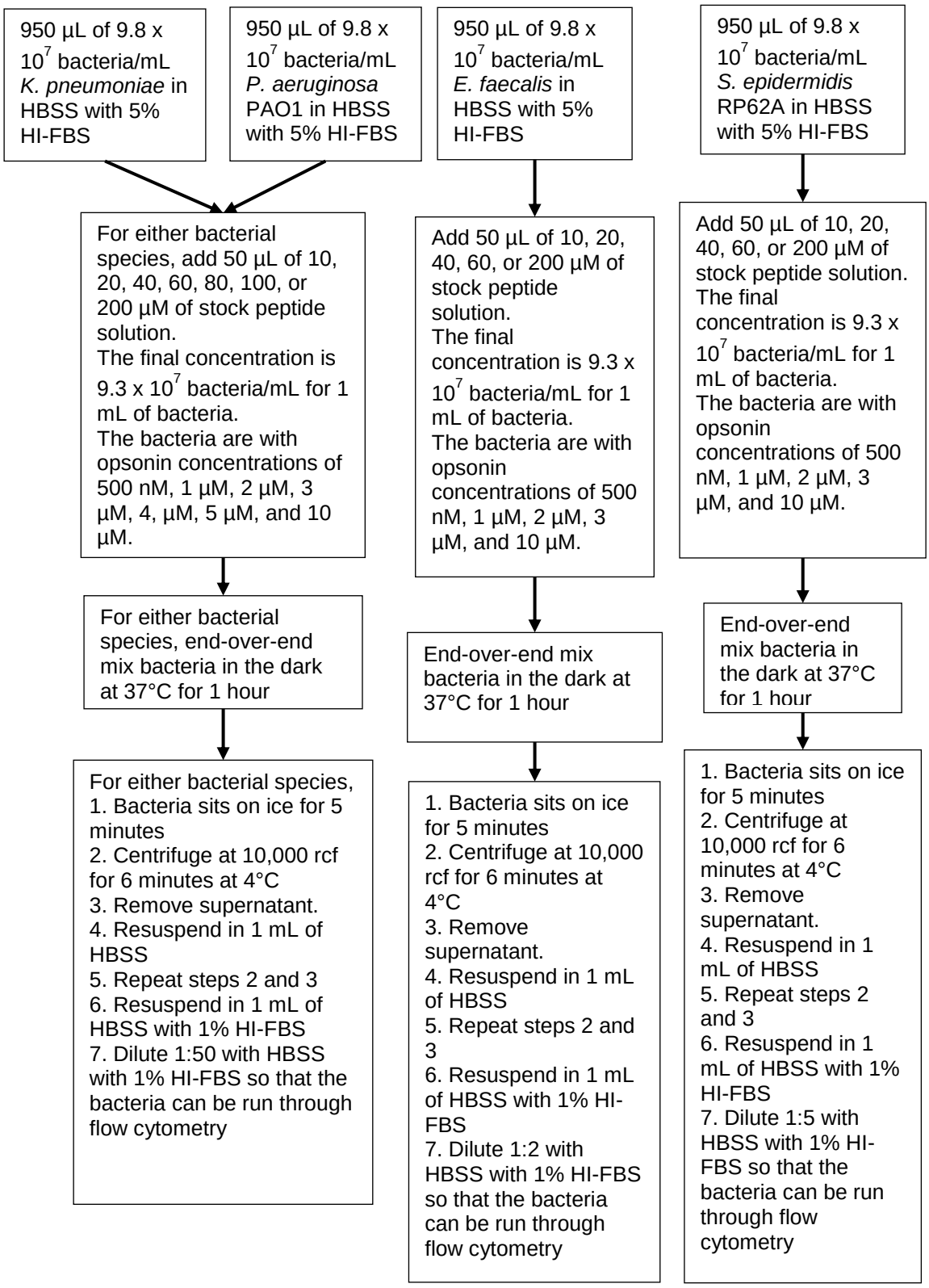

Figure 2.3.2.1: A flowchart detailing how samples of the four bacterial species were opsonized and prepared for flow cytometry

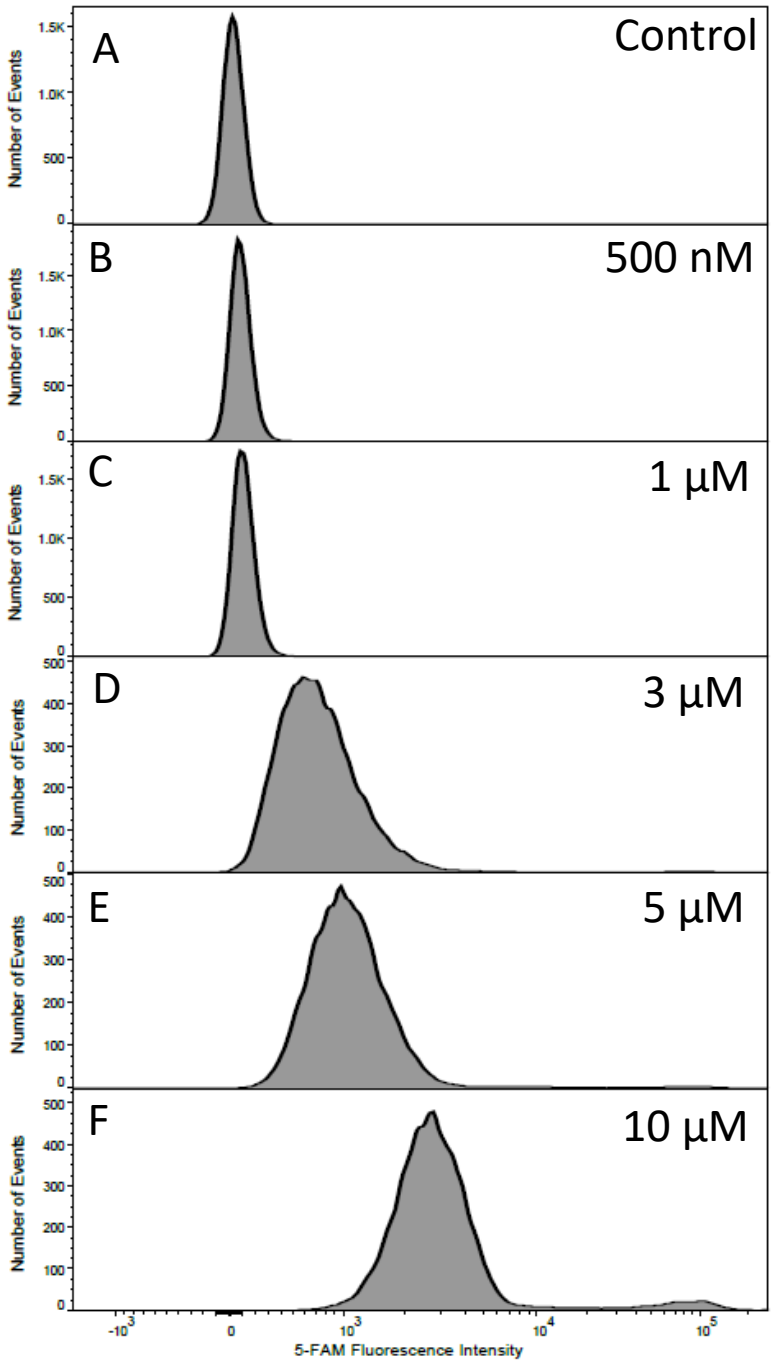

Figure 2.4.1: 5-FAM fluorescence intensity histograms for individual *K. pneumoniae* samples with 0 nM (A), 500 nM (B), 1 µM (C), 3 µM (D), 5 µM (E), and 10 µM (F) of 5-FAM labeled opsonin

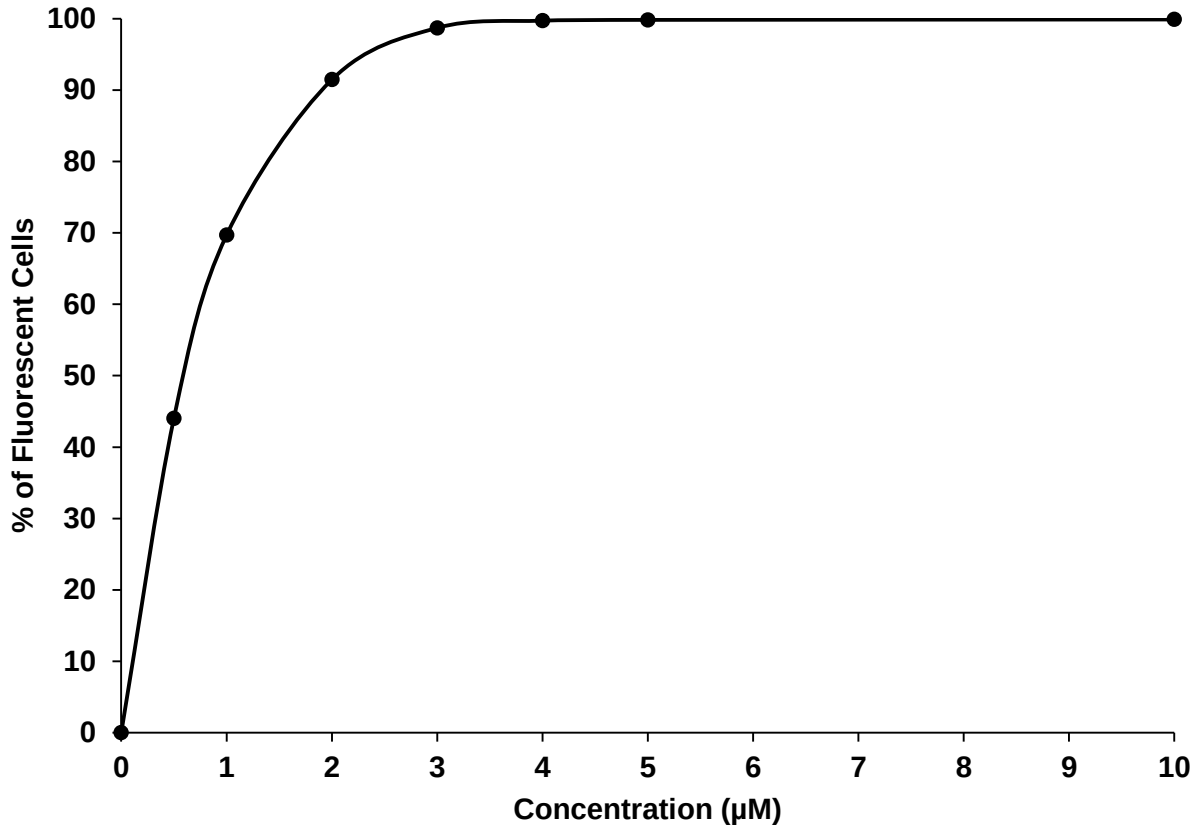

Figure 2.4.2: Percentage of fluorescent cells in relation to applied opsonin concentration for 1 mL of 9.3 x 10^7 *K. pneumoniae* cells/mL

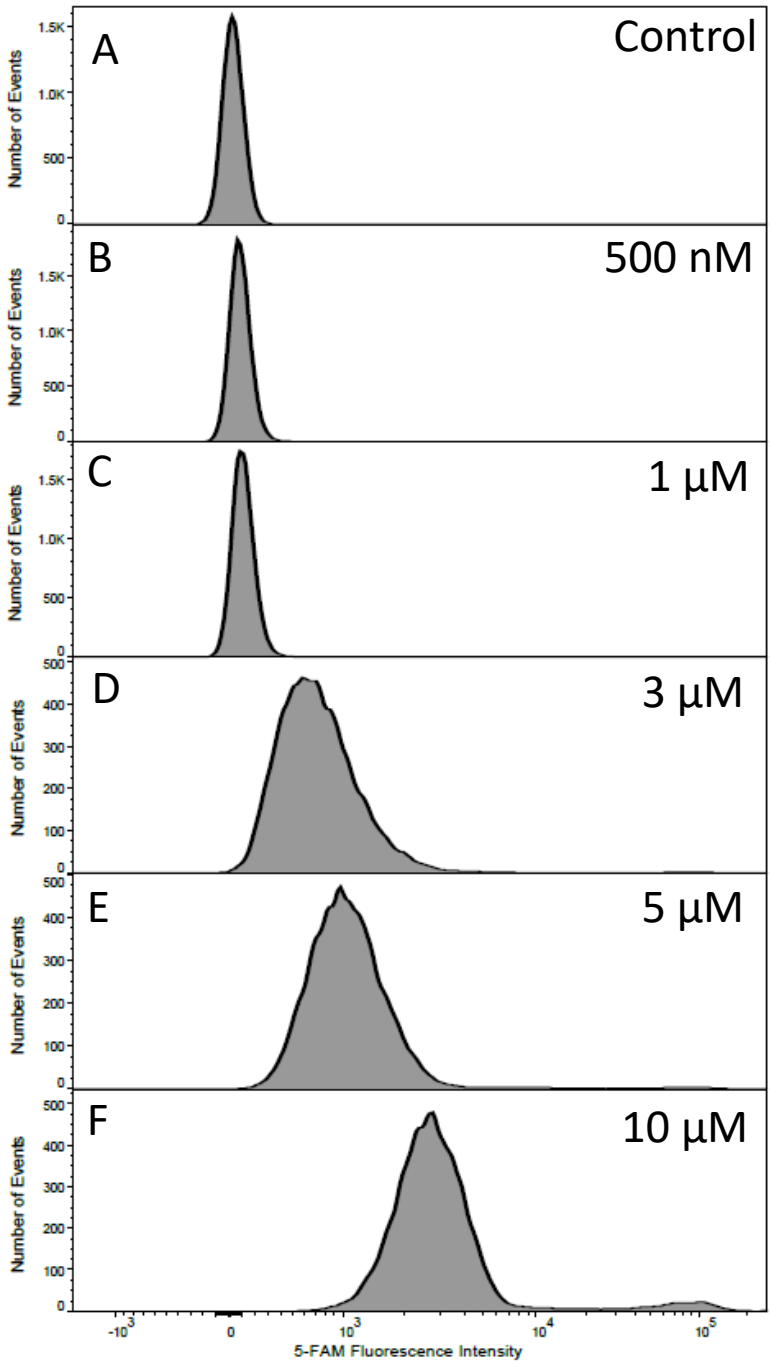

Figure 2.4.3: 5-FAM fluorescence intensity histograms for individual *P. aeruginosa* PAO1 samples with 0 nM (A), 500 nM (B), 1 µM (C), 3 µM (D), 5 µM (E), and 10 µM (F) of 5-FAM labeled opsonin

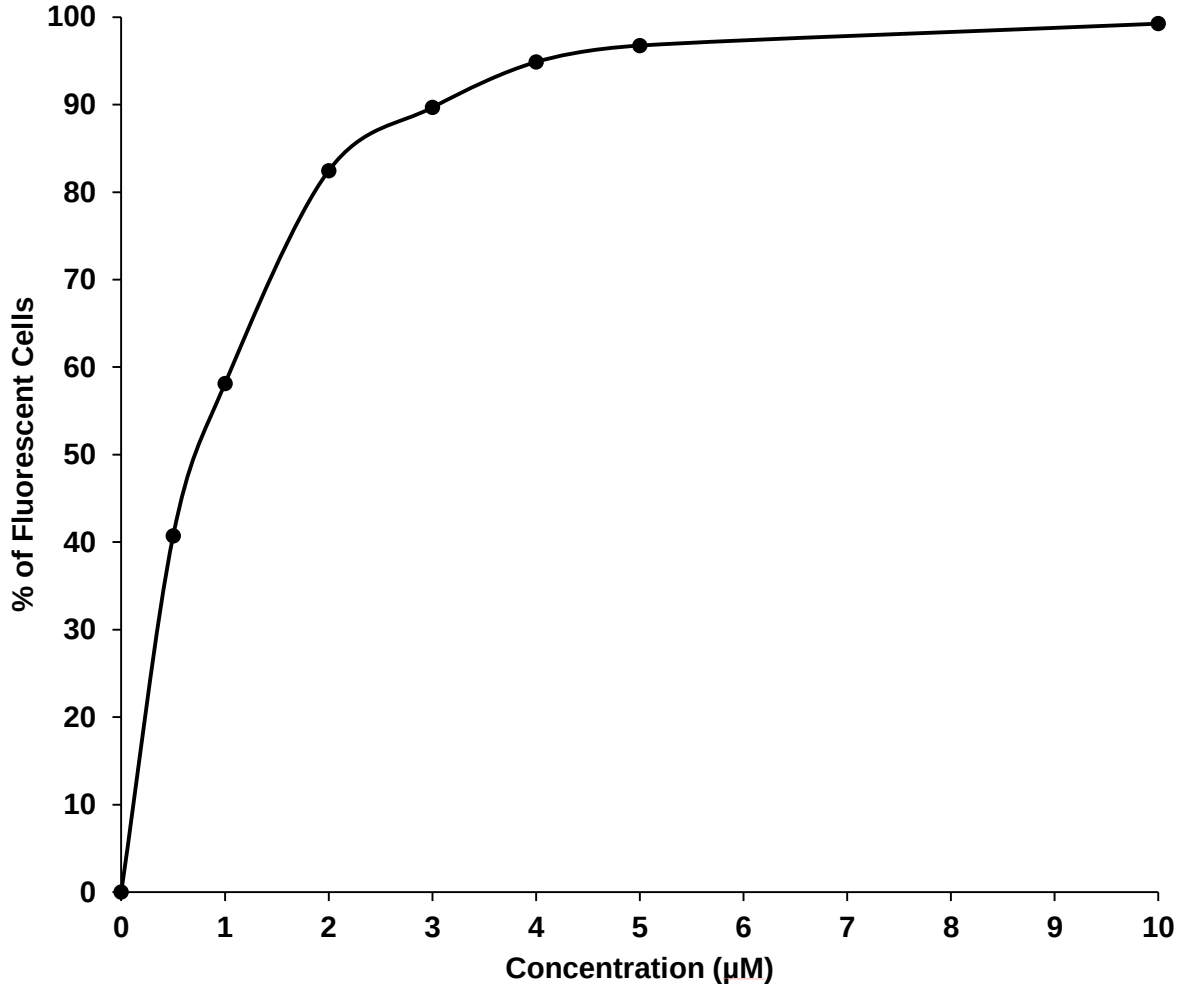

Figure 2.4.4: Percentage of fluorescent cells in relation to applied opsonin concentration for 1 mL of 9.3 x 10^7 *P. aeruginosa* PAO1 cells/mL

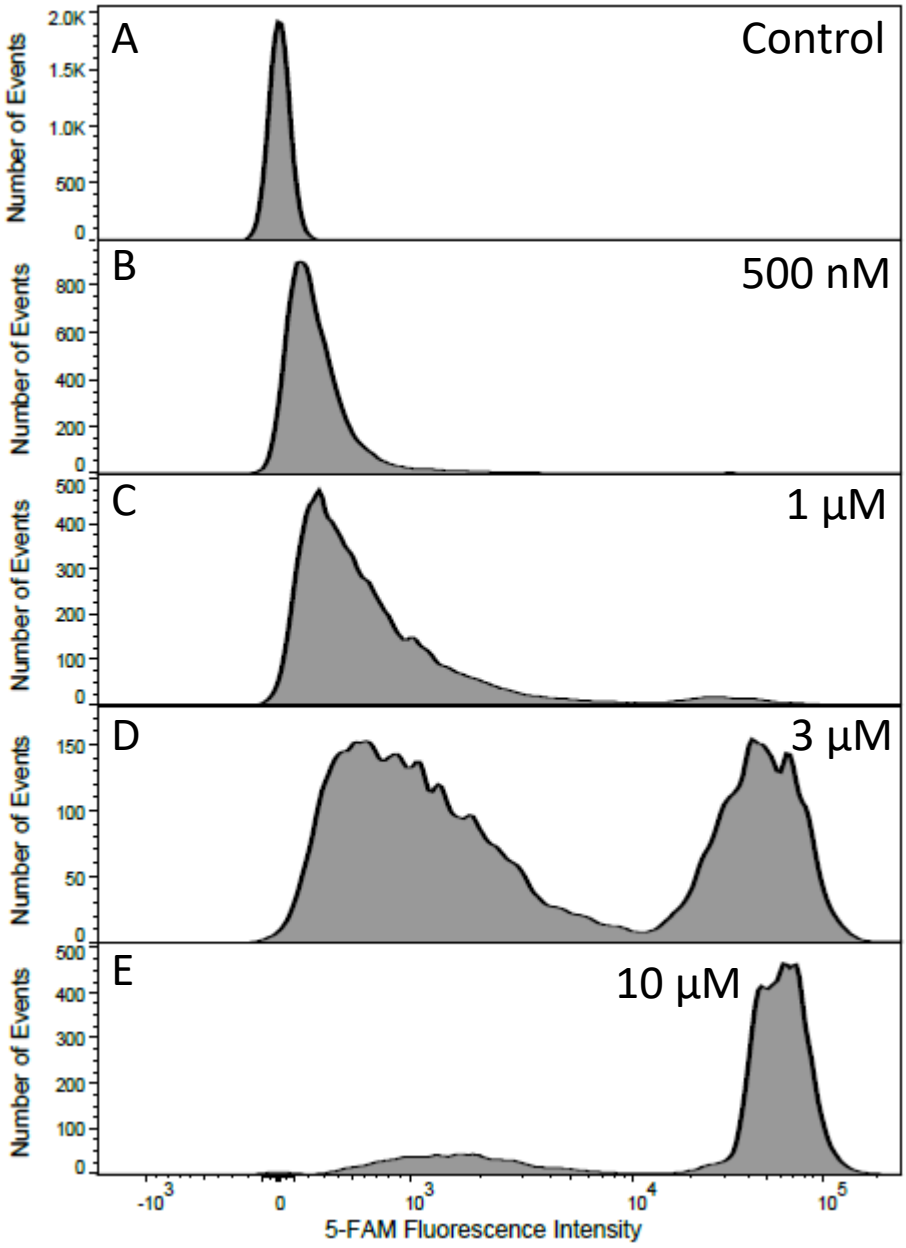

Figure 2.4.5: 5-FAM fluorescence intensity histograms for individual *S. epidermidis* RP62A samples with 0 nM (A), 500 nM (B), 1 µM (C), 3 µM of (D), 10 µM (E) of 5-FAM labeled opsonin

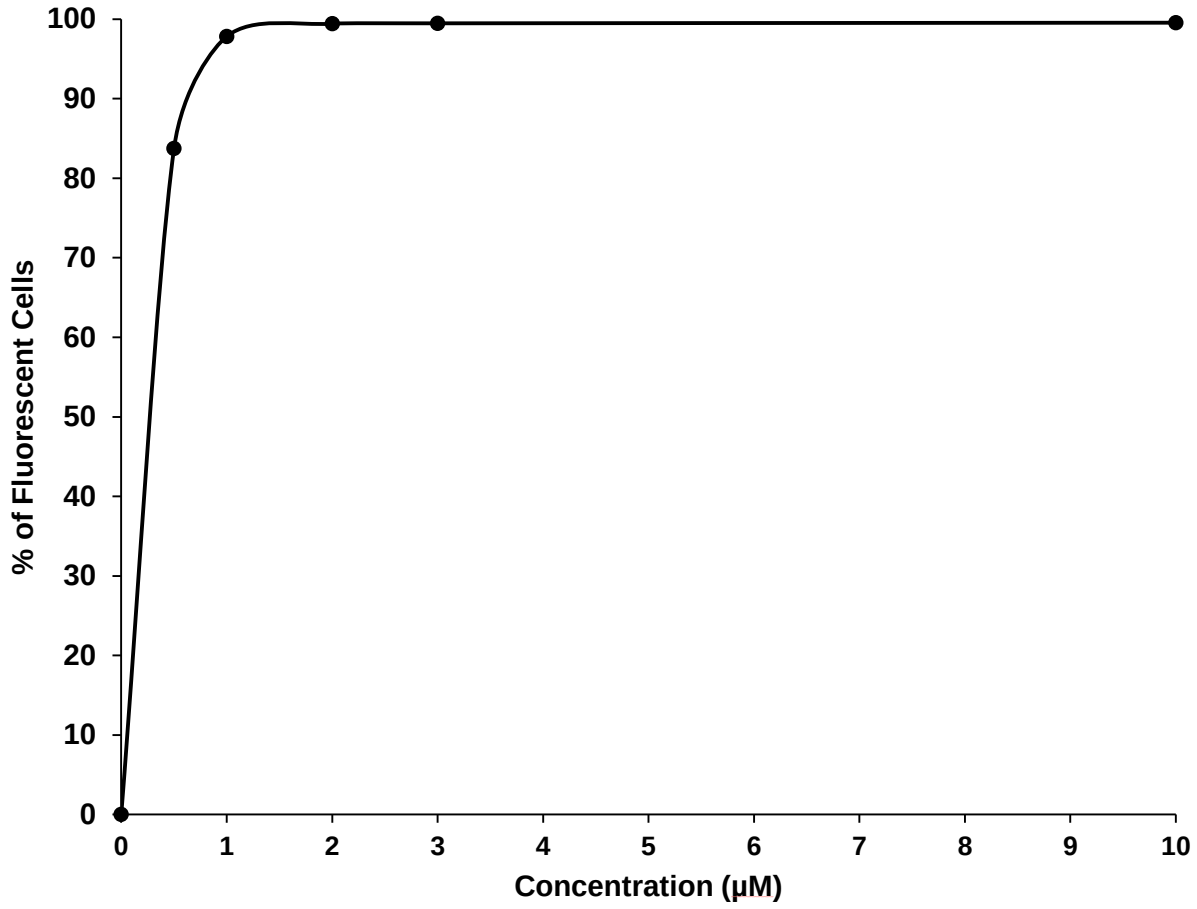

Figure 2.4.6: Percentage of fluorescent cells in relation to applied opsonin concentration for 1 mL of 9.3 x 10^7 *S. epidermidis* RP62A cells/mL

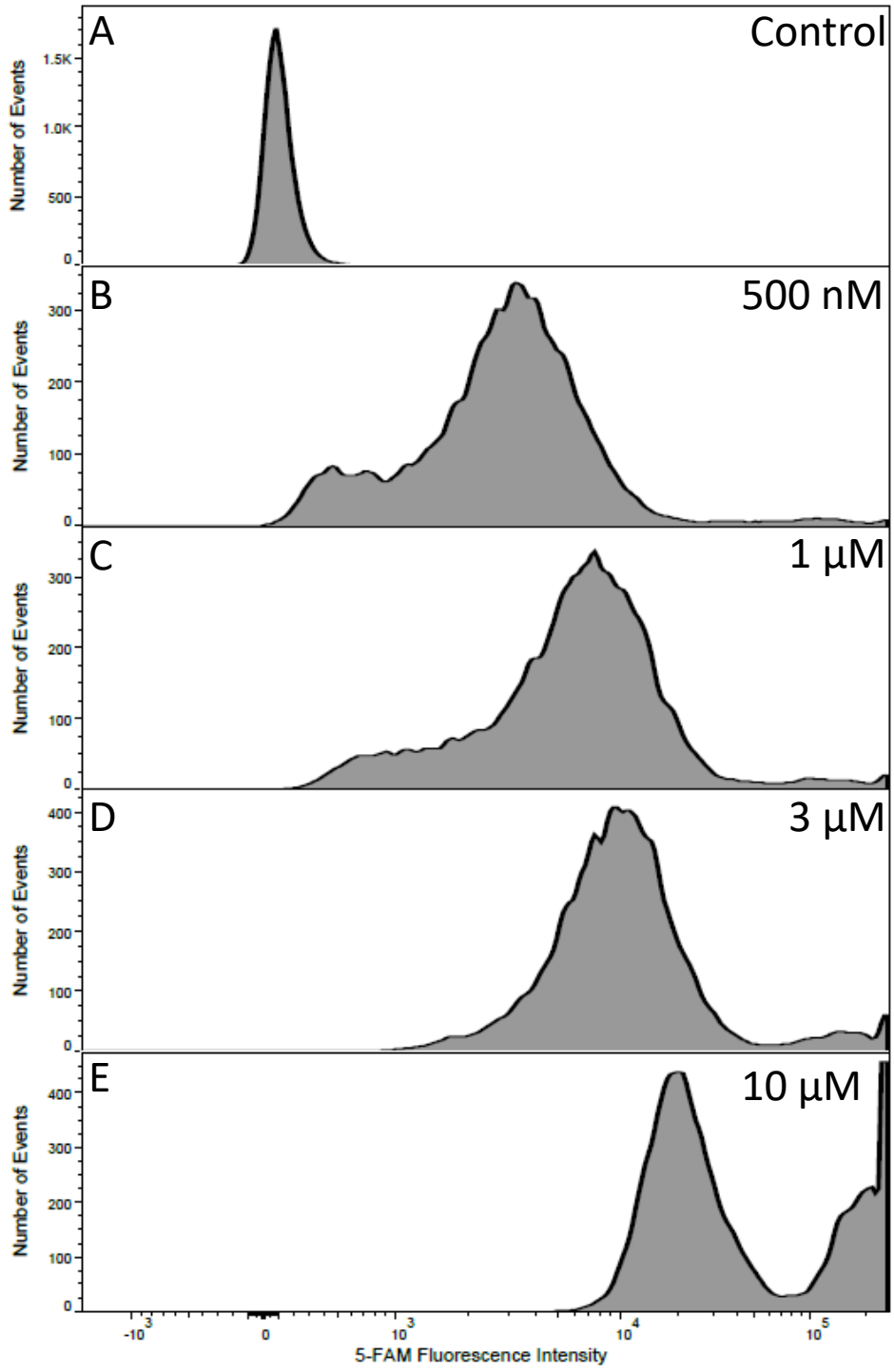

Figure 2.4.7: 5-FAM fluorescence intensity histograms for individual *E. faecalis* samples with 0 nM (A), 500 nM (B), 1 µM (C), 3 µM of (D), 10 µM (E) of 5-FAM labeled opsonin

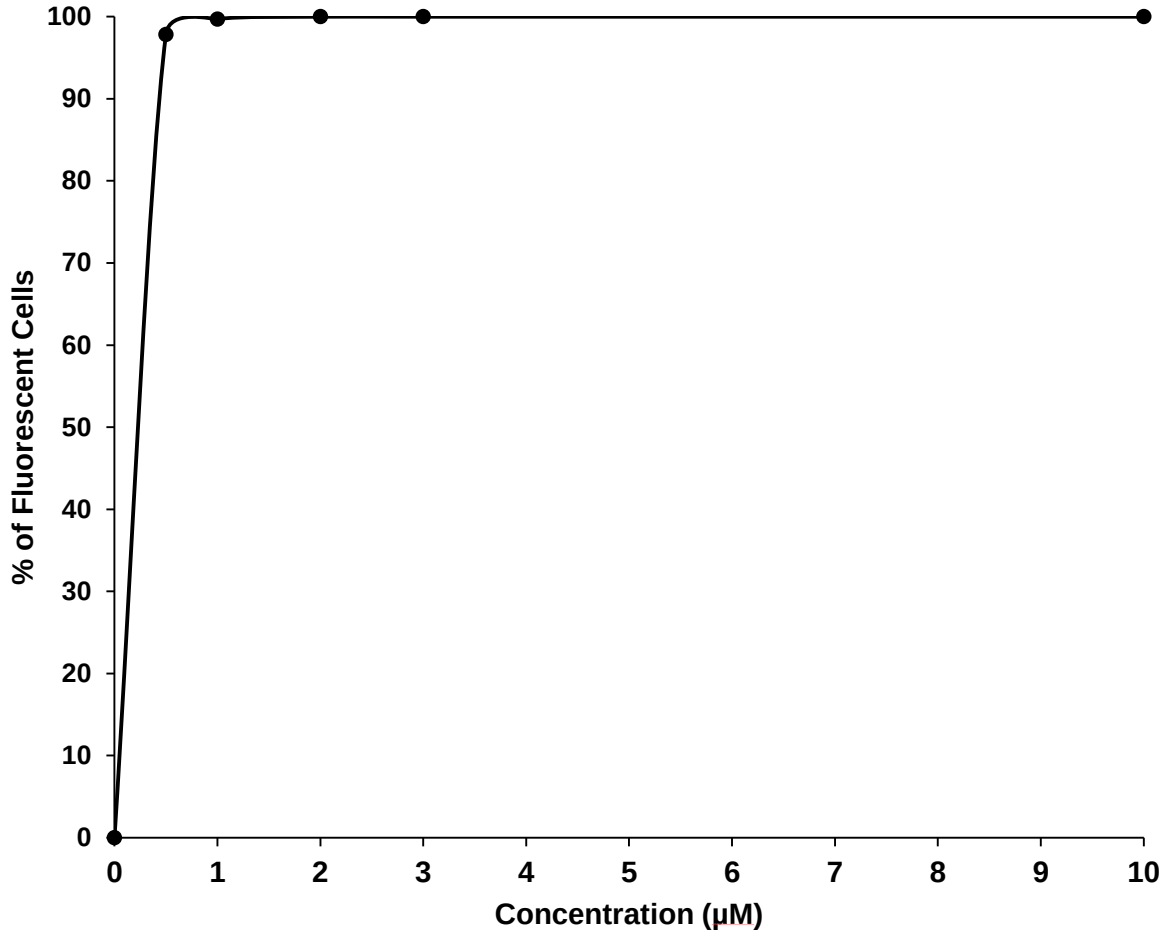

Figure 2.4.8: Percentage of fluorescent cells in relation to applied opsonin concentration for 1 mL of 9.3 x 10^7 *E. faecalis* cells/mL

Chapter 3: Binding of 5-FAM Labeled Artificial Opsonin to RAW 264.7 Macrophages

3.1 Abstract

In this chapter, the degree to which the artificial opsonin binds to the RAW 264.7 mouse macrophage cell line was examined. 1 mL of 8.0 x 10^5 cells/mL was incubated with 5-FAM labeled artificial opsonin in a fashion similar to the bacterial binding assay of Chapter 2. Flow cytometry was used to assess the amount of binding of the opsonin to the macrophages. By increasing the applied opsonin concentration, the artificial opsonin was able to saturate the RAW 264.7 macrophages. 99.5% of the macrophages exhibited binding at an opsonin concentration of 50 nM and greater.

3.2 Introduction

The goal of the artificial opsonin is to provide a dual linkage to both bacteria and macrophages. Chapter 2 reports on the ability of the artificial opsonin to bind to various bacterial species. Here in chapter 3, the extent to which varying concentrations of 5-FAM labeled opsonin bind to RAW 264.7 cells is examined.

RAW 264.7 cells were used because they are appropriate models of macrophages. These cells can perform pinocytosis and phagocytosis. Furthermore, they can eliminate pathogens through antibody-dependent cellular toxicity [50].

3.3 Materials and Methods

3.3.1 Preparation of RAW 264.7 Culture

1.1×10^6 RAW 264.7 cells in Dulbecco's Modified Eagle Medium (DMEM, Gibco) with 10% HI-FBS (Gibco) were plated in a Corning T-75 flask and grown at 37°C with 5% CO_2 for three days. On the third day, the cells were used for the opsonin binding assay. The medium was removed and replaced with 5 mL of HBSS with 5% HI-FBS. With a cell scraper, cells were scraped off the flask and into the 5 mL of HBSS with 5% HI-FBS. The 5 mL with cells was pipetted into a 15 mL centrifuge tube and centrifuged at 950 rpm for 6 minutes in a Jouan Cr-412 centrifuge. The supernatant was removed, and the cell pellet was resuspeneded in 5 mL of HBSS with 5% HI-FBS. The centrifugation and extraction of supernatant steps were repeated once. Then, the cell pellet was resuspended in 10 mL of HBSS with 5% HI-FBS. The concentration of viable cells and cell viability were determined by microscopically examining a 1:1 mixture of cells in HBSS with 5% HI-FBS and 0.4% trypan blue solution (Sigma-Aldrich) with a hemocytometer [51]. 8.0×10^5 cells and HBSS with 5% HI-FBS were added to 1.5 mL centrifuge tubes to reach a total volume of 950 µL at a concentration of 8.4×10^5 cells/mL. The steps described in this subsection are illustrated in Figure 3.3.1.1.

3.3.2 Opsonin binding to RAW 264.7 Cells

0.2 mg of lyophilized 5-FAM labeled opsonin (GenScript) was dissolved in 1 mL of ultrapure water. Stock solutions of 1, 2, 5, 10, and 20 µM were made from the base opsonin solution. Then, 50 µL of these stock solution were individually pipetted into the 1.5 mL centrifuge tubes containing the RAW 264.7 cells. As a result, the final 5-FAM labeled opsonin concentrations of 50 nM, 100 nM, 250 nM, 500 nM, and 1 µM were mixed with 1 mL of 8.0×10^5 cells/mL. For

the controls, 50 µL of ultrapure water was added. The RAW cell tubes with ultrapure water or opsonin were end-over-end mixed in the dark at 37°C for 20 minutes.

Then, all samples were put on ice for 5 minutes. Using an Eppendorf 5417c centrifuge, the cells were centrifuged at 750 rcf for 6 minutes at 4°C. The supernatant was removed, and the cell pellets were resuspended in 1 mL of chilled HBSS. The centrifugation and supernatant extraction steps were repeated one. Afterwards, the RAW cell pellets were resuspended in 1 mL of HBSS with 1% HI-FBS. The steps for this subsection are illustrated in Figure 3.3.2.1.

3.3.3 Flow Cytometry

The 1 mL cell suspensions were transferred into 5 mL flow cytometry tubes, and the flow cytometry tubes were placed on ice. All the samples were analyzed on a BD Biosciences LSRII flow cytometer. One color flow cytometry was utilized because the opsonin was the only fluorescent component that needed to be recorded. 10,000 events were collected based on two gating parameters: side scatter area versus forward scatter area and forward scatter width versus forward scatter area. All the voltages were kept the same from experiment to experiment to ensure that all experiments could be compared with one another.

3.3.4 Data Analysis

FlowJo software version 10.1 (Treestar) was used for data analysis. The events collected were gated based on side scatter area versus forward scatter area and forward scatter width versus forward scatter area. The gated samples' 5-FAM fluorescence histograms were used to determine the extent of binding of the opsonin to the RAW cells. With the SE Dymax algorithm in the FlowJo software, individual experimental samples were compared to every individual control sample used throughout the experiments. Based on a sample size of n = 4, the average of all the

SE Dymax values for a certain concentration was used to provide an overall assessment of the percentage of fluorescent cells with bound opsonin for a given applied opsonin concentration.

From the average percentage of macrophages showing fluorescence at a specific concentration, the number of macrophages in each sample, and Avogadro's number, the number of opsonins bound to one macrophage was determined. The concentration of applied artificial opsonin was converted into moles, and the moles was converted into number of molecules with Avogadro's number. Based on the average percentage of macrophages with fluorescence at specific opsonin concentrations and the number of macrophages in each sample, the number of macrophages that were fluorescent at a given opsonin concentration was calculated. Afterwards, the number of opsonin molecules bound to one macrophage was determined.

3.4 Results

Based on the histograms of all the samples, an increase in applied opsonin concentration correlated to an increase in cell 5-FAM fluorescence. As the concentration of applied opsonin increased, the single-peak curve in the 5-FAM fluorescence histograms shifted to the right towards higher values of 5-FAM fluorescence. This is shown in Figure 3.4.1.

According to the values obtained from SE Dymax, a vast majority of RAW cells showed binding $\geq$ 50 nM. At 50 nM, 99.5% of the RAW cells had bound to the opsonin At 250 nM, 100% of the RAW cells showed binding. However, this does not mean that the cells were fully saturated. Figure 3.4.2 show the relationship between percentage of fluorescent cells and applied opsonin concentration for 1 mL of 8.0×10^5 RAW 264.7 cells/mL.

The number of artificial opsonin molecules bound to one RAW 264.7 macrophage was 2.86×10^8 molecules/cell.

3.5 Discussion

On average, the amount of opsonin bound to RAW 264.7 cells increased as the applied opsonin concentration increases. While 250 nM indicates that 100% of the RAW cells showed binding to the opsonin, as shown in Figure 3.4.2, Figure 3.4.1 illustrates that increasing the applied opsonin concentration can increase the amount of binding observed. Nevertheless, the results indicate that the artificial opsonin shows affinity towards RAW 264.7 macrophages.

3.6 Conclusion

The assay described in this chapter illustrates that the artificial opsonin has an affinity towards RAW 264.7 cells. 100% of the macrophages exhibited binding at ≥ 250 nM, but this does not indicate that the cells were fully saturated with opsonin. Fluorescence increased with increasing opsonin concentration, signifying that the macrophages were able to bind to opsonin with higher applied opsonin concentrations.

Based on the results from Chapter 2 and 3, more opsonin is needed to saturate 9.3×10^7 gram-negative and gram-positive bacteria as opposed to 8.0×10^5 RAW 264.7 cells. Specifically, 3 µM of opsonin is 9.3×10^7 *K. pneumoniae* cells, while 250 nM of opsonin is needed to saturate RAW 264.7 cells. Thus, *K. pneumoniae* that has been opsonized with 5 µM should have sufficient amounts of opsonin that can bind to RAW 264.7 cells.

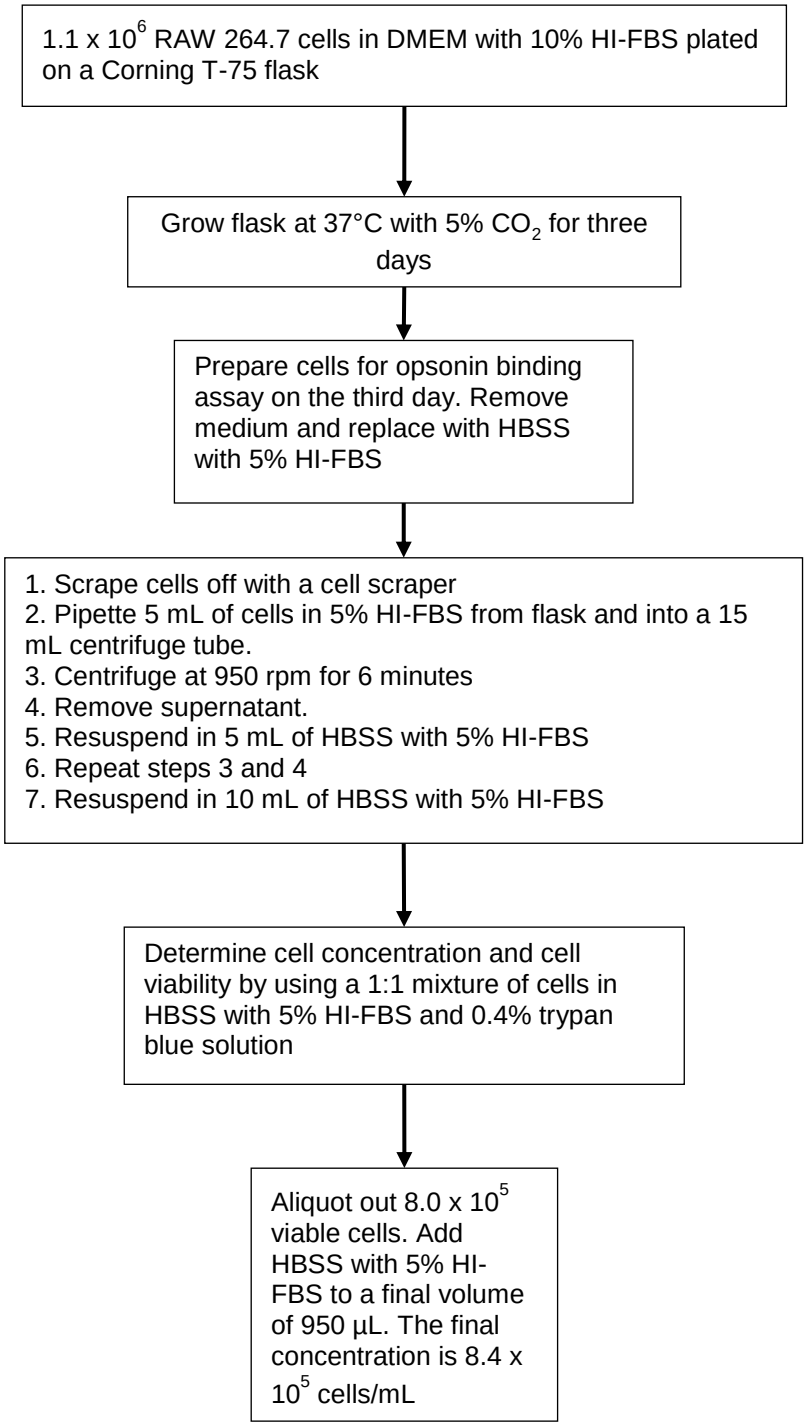

Figure 3.3.1.1: A flowchart describing how the RAW 264.7 culture was prepared for the opsonin binding assay

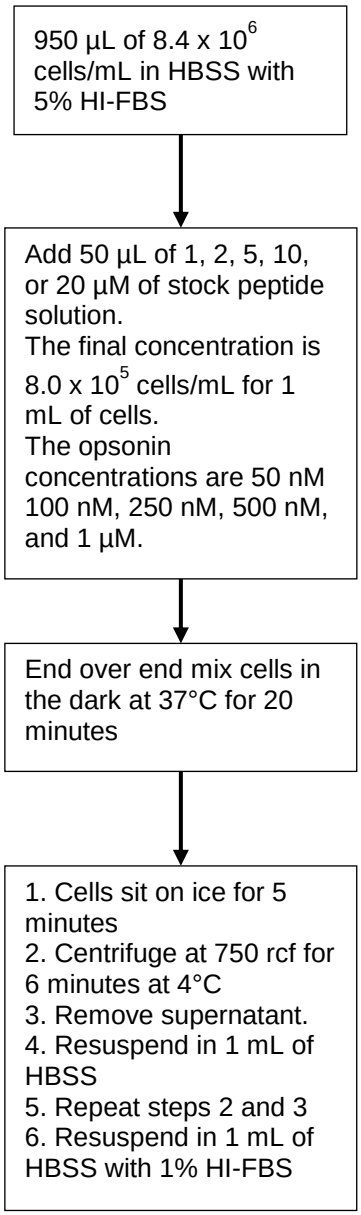

Figure 3.3.2.1: A flowchart detailing how samples of RAW 264.7 cells were bound to the opsonin

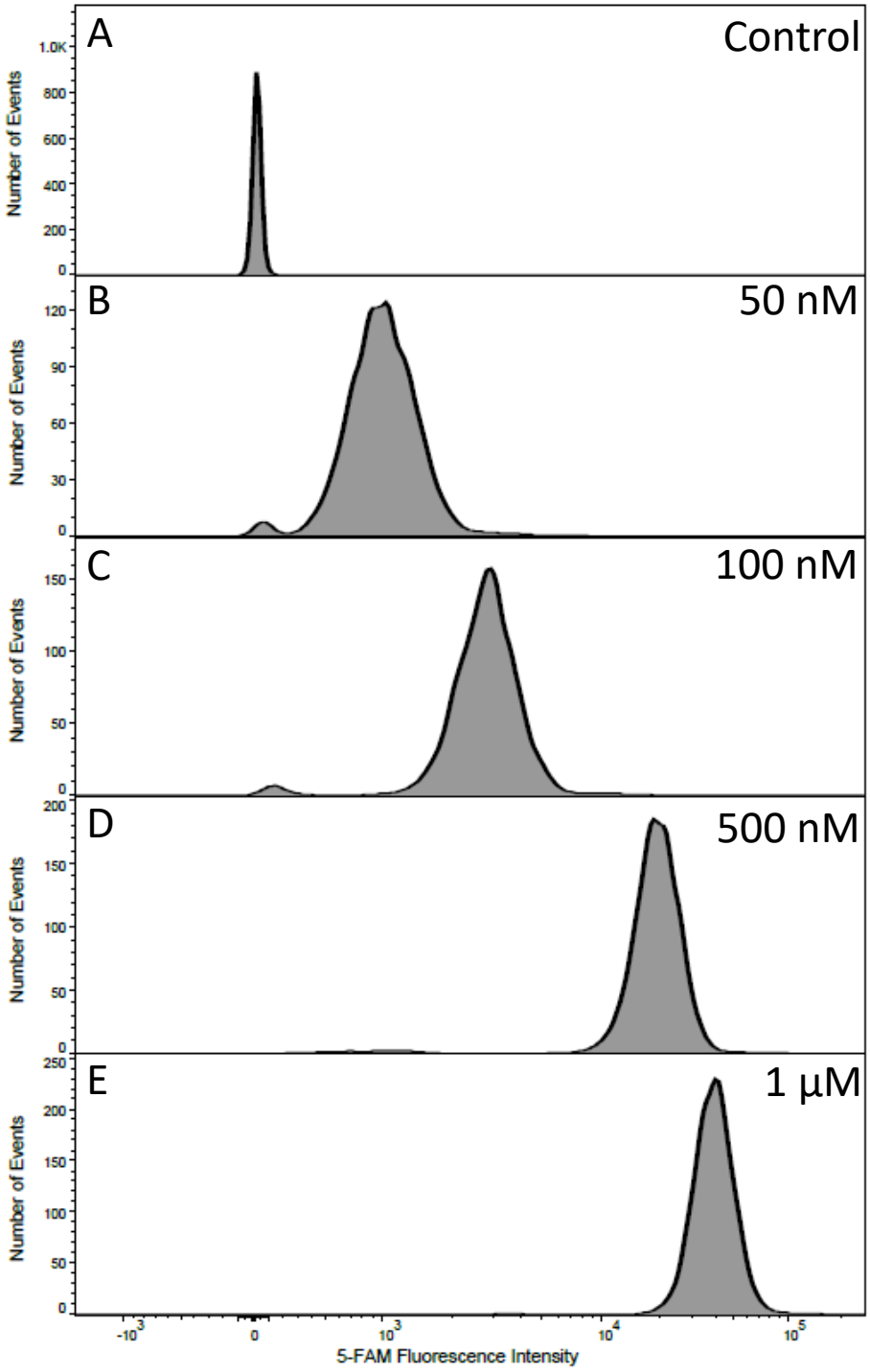

Figure 3.4.1: 5-FAM fluorescence intensity histograms for individual RAW 264.7 samples with 0 nM (A), 50 nM (B), 100 nM (C), 500 nM of (D), and 1 µM (E) of 5-FAM labeled opsonin

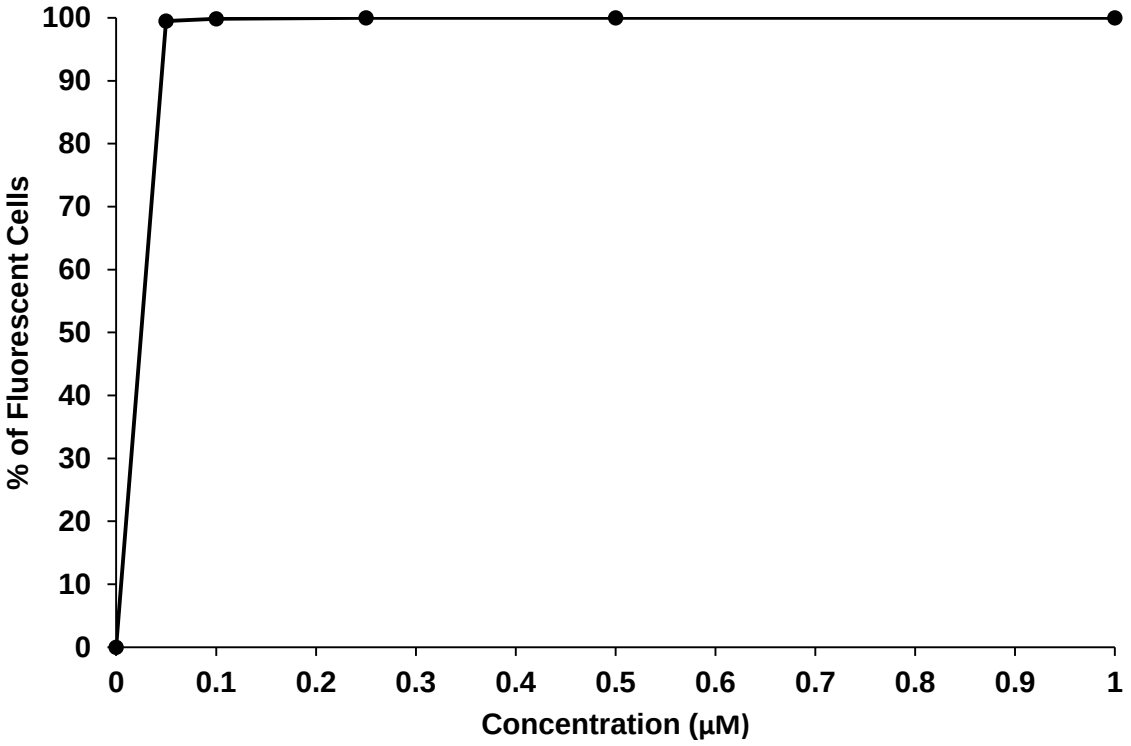

Figure 3.4.2: Percentage of fluorescent cells in relation to applied opsonin concentration for 1 mL of 8.0 x 10^5 RAW 264.7 cells/mL

Chapter 4: Opsonin Efficacy to enhance Phagocytosis of *K. pneumoniae* bacteria

4.1 Abstract

This chapter reports on studies to determine if the artificial opsonin can indeed enhance phagocytosis of bacteria. 8.0×10^6 opsonized or non-opsonized fluorescently-labeled bacteria were mixed with 8.0×10^5 RAW 264.7 cells. Trypan blue was used to differentiate between fluorescent bacteria adherent to the exterior of macrophages and phagocytosed, fluorescent bacteria residing within macrophages. Fluorescence was detected by a plate reader. With a sample size of four, macrophages were capable of phagocytosing 59.85% and 46.29% of non-opsonized and opsonized bacteria, respectively. Using a two-sided t-test, the calculated t and p values were 0.7623 and 0.4748, respectively. As a result, the artificial opsonin did not exhibit a statistical enhancement of bacterial phagocytosis.

4.2 Introduction

In this chapter, the extent of phagocytosis, defined as the percentage of bacteria phagocytosed, by RAW 264.7 cells of *Klebsiella pneumoniae*, whether opsonized or not, will be examined. As discussed in Chapter 1, the opsonin includes di-tuftsin, a tetrapeptide of the IgG leukokinin, and YI13WF, a peptide which can bind to LPS on gram-negative bacterial membranes. Hypothetically, the opsonin will bind to *K. pneumoniae* through YI13WF and to macrophages through di-tuftsin. In doing so, the opsonin should enhance phagocytosis.

Since phagocytosis is not guaranteed to be 100%, the fluorescence between non-phagocytosed bacteria and phagocytosed bacteria must be distinct. Trypan blue has traditionally

been used to quench extracellular FITC fluorescence in phagocytosis assays since trypan blue cannot penetrate viable cell membranes [52-54].

4.3 Materials and Methods

4.3.1 Preparation of *K. pneumoniae* for Fluorescent Labeling

A colony of *K. pneumoniae* from a LB Miller agar plate was grown in 10 mL of LB Miller medium (Fisher BioReagents) for 16 hours at 37°C and 180 rpm in a New Brunswick Scientific Excella E24 incubator shaker. After 16 hours, 9.4 mL of the liquid culture was centrifuged at 3650 rpm for 13 minutes in a Thermo Sorvall Legend Rt+ centrifuge. Then, the supernatant was removed, and the bacterial pellet was resuspended in 9.4 mL of sterile HBSS. The centrifugation, supernatant removal, and resuspension steps were repeated once to remove any residual medium.

With the second wash step complete, the optical density at 600 nm (OD600) of the bacteria was measured using a Genesys 10S UV-Vis spectrophotometer (ThermoFisher). Based on the OD600 readings and a calibration curve previously made relating OD600 to concentration of *K. pneumoniae* (bacteria/mL), the concentration of the 9.4 mL bacterial suspension was determined. 7 1.5 mL centrifuge tubes were filled with 1 mL bacterial suspensions with a concentration of 1.86×10^8 cells/mL. All of the steps described in this section is illustrated in Figure 4.3.1.1.

4.3.2 Fluorescently Labeling *K. pneumoniae*

All 7 tubes with bacteria received 10 µL of a 10 mg FITC (ThermoFisher) per 1 mL of DMSO (Sigma-Aldrich) solution. All tubes were covered in foil and end-over-end mixed at room temperature in the dark for 30 minutes.

Then, bacterial suspensions were centrifuged at 10,000 rcf for 6 minutes at room temperature with an Eppendorf 5417c centrifuge. The supernatants were removed, and the

bacterial pellets were resuspended in 1 mL of HBSS. A second wash was performed to remove residual unbound FITC. After the second wash, the bacterial pellets were resuspended with 1 mL of HBSS with 5% HI-FBS. Each tube with FITC-labeled bacteria contained 1 mL of 1.9 x 10^8 cells/mL.

3 tubes with FITC-labeled bacteria, deemed as tube set A, were used to examine the extent to which trypan blue quenches FITC. The remaining 4 tubes with FITC-labeled bacteria, deemed as tube set B, were used as potential sources of bacteria for the phagocytosis assay. The steps described in 4.3.2 are presented in Figure 4.3.2.1.

4.3.3 Preparation of FITC-labeled *K. pneumoniae* for Opsonization

Since opsonin binding assays were carried out with 1 mL of 9.3 x 10^7 bacteria/mL, the contents of the seven tubes containing FITC-labeled bacteria were divided in two. For tubes in tube set B, 500 µL from each tube were aliquoted into a new 1.5 mL tubes. As a result, there were 8 tubes, each with 500 µL of 1.9 x 10^8 FITC-labeled bacteria/mL. 4 of the 8 tubes, deemed as tube set B1, will have FITC-labeled bacteria that will not be opsonized. The remaining 4 tubes, deemed as tube set B2, will have FITC-labeled bacteria that will be opsonized. Afterwards, 450 µL of HBSS with 5% HI-FBS was added to tubes in set B1 and B2. As a result, B1 and B2 had tubes filled with 950 µL bacterial suspensions at a concentration of 9.8 x 10^7 FITC-labeled bacteria/mL. The steps for generating sets B1 and B2 are illustrated in Figure 4.3.3.1.

For the remaining 3 tubes, 2 250 µL aliquots from each tube was transferred into 2 2 mL centrifuge tubes. As a result, there were 6 tubes, each with 250 µL of 1.9 x 10^8 FITC-labeled bacteria/mL. 3 of the 6 tubes, deemed as tube set A1, had FITC-labeled bacteria that would not be quenched with trypan blue. The remaining 3 tubes, deemed as tube set A2, had FITC-labeled bacteria that would be quenched with trypan blue. Afterwards, 750 µL of HBSS was added to

tubes in set A1 and A2. As a result, A1 and A2 had tubes filled with 1 mL bacterial suspensions at a concentration of 4.6 x 10^7 FITC-labeled bacteria/mL. Then, sets A1 and A2 were placed in a foil covered box, and the box was put into a 4°C fridge. The steps for generating sets A1 and A2 are illustrated in Figure 4.3.3.1.

4.3.4 Opsonization of FITC-labeled *K. pneumoniae*

With the subdivision of the bacteria complete, a 100 µM stock solution of artificial opsonin (GenScript) was made. Tubes in set B1 received 50 µL of ultrapure water, while tubes in set B2 received 50 µL of the 100 µM solution of artificial opsonin. As a result, tubes in set B1 and B2 had 1 mL of 9.3 x 10^7 FITC-labeled bacteria/mL. Tubes in set B2 contained a final opsonin concentration of 5 µM. All 8 tubes were end-over-end mixed in the dark at 37°C for one hour. After one hour, the tubes were put on ice until the steps for preparing the RAW 264.7 cells (described in section 4.3.5) were complete. When the steps in section 4.3.5 were completed, the bacterial suspensions inside tubes from sets B1 and B2 were centrifuged at 10,000 rcf for 6 minutes. Once complete, the supernatant was removed and the bacterial pellets were resuspended in 1 mL of HBSS with 5% HI-FBS.

The fluorescence of opsonized and non-opsonized FITC-labeled bacteria were compared by plating the bacterial suspensions on a 96 well black, clear flat bottom polystyrene non-treated microplate (Corning). Bottom readings of the plate were taken with an EnSight Multimode Microplate Reader (PerkinElmer). Based on the fluorescence readings, one tube from sets B1 and B2 (2 tubes total) were selected to be the sources of non-opsonized and opsonized bacteria, respectively, for the phagocytosis assay. The steps described in this section are illustrated in Figure 4.3.4.1.

4.3.5 Preparation of RAW 264.7 cells for Phagocytosis

1.1 x 10^6 RAW 264.7 cells were plated in a Corning T-75 flask and grown in DMEM (Gibco) with 10% HI-FBS (Gibco) at 37°C with 5% CO_2 for 3 days. On the 3rd day, the RAW 264.7 cells were prepared for the phagocytosis assay. The medium was removed and replaced with 5 mL of HBSS with 5% HI-FBS. The cells were scraped off the flask with a cell scraper, and the 5 mL with cells was centrifuged at 950 rpm for 6 minutes in a Jouan Cr-412 centrifuge. Then, the supernatant was removed and the cell pellet was resuspeneded in 5 mL of HBSS with 5% HI-FBS. The centrifugation and removal of supernatant steps were repeated once. Afterwards, the cell pellet was resuspended in 10 mL of HBSS with 5% HI-FBS. The concentration of viable cells and cell viability were determined by microscopically examining a 1:1 mixture of cells in HBSS with 5% HI-FBS and 0.4% trypan blue solution with a hemocytometer [51].

8.0 x 10^5 viable cells and HBSS with 5% HI-FBS were added to 10 2 mL tubes to reach a total volume of either 1 mL or 914 µL. 6 tubes were filled up to a volume of 914 µL because they would be used for the phagocytosis assay. 3 of the 6 tubes, deemed as tube set C, contained 914 µL of 8.8 x 10^5 cells/mL purposed for phagocytosing non-opsonized, FITC-labeled bacteria. The remaining 3 tubes, deemed as tube set E, contained 914 µL of 8.8 x 10^5 cells/mL purposed for phagocytosing opsonized, FITC-labeled bacteria. 4 of the 10 tubes, deemed as tube set G, contained 1 mL of 8.0 x 10^5 cells/mL purposed for determining the fluorescence of RAW 264.7 cells with and without quenching by trypan blue. While the RAW 264.7 cells may not be inherently fluorescent, trypan blue affects the fluorescence intensity outputted due to trypan blue's dark blue appearance and quenching capabilities. The steps described in this section are illustrated in Figure 4.3.5.1.

4.3.6 Phagocytosis of Opsonized or Non-opsonized FITC-labeled *K. pneumoniae* by RAW 264.7 cells

The bacteria and RAW cells were mixed thoroughly before they were used. All tubes in set C received 86 µL containing 8.0 x 10^6 non-opsonized, FITC-labeled bacteria. All tubes in set E received 86 µL containing 8.0 x 10^6 opsonized, FITC-labeled bacteria. As a result, 1 mL of 8.0 x 10^5 cells/mL were mixed with either 8.0 x 10^6 non-opsonized or opsonized FITC-labeled bacteria. The multiplicity of infection (MOI) for these studies, defined as the ratio of bacteria to macrophages, was 10.

Afterwards, tubes in sets C, E, and G were end-over-end mixed in the dark at 37°C for 20 minutes. After 20 minutes, all the tubes were put on ice for five minutes. Then, tubes in set C, E, and G, were mixed thoroughly before being subdivided into two. 500 µL from each tube was transferred to a different 2 mL tube. As a result, the subdivision of C, E, and G, led to the formation of tube sets D, F, and H, respectively. 500 µL of chilled HBSS was added to all of the tubes. In the end, tubes in set C and D had 1 mL of 4.0 x 10^5 cells/mL that phagocytosed non-opsonized, FITC-labeled bacteria. Tubes in set E and F contained 1 mL of 4.0 x 10^5 cells/mL that phagocytosed opsonized, FITC-labeled bacteria. Tubes in set G and H contained 1 mL of 4.0 x 10^5 cells/mL. Tubes in D, F, and H were purposed as replicates of tubes in C, E, and G that would be quenched with trypan blue.

The cell suspensions in sets C, D, E, F, G, and H were centrifuged at 750 rcf and 4°C for 9 minutes. Once the centrifugation was complete, 650 µL of the supernatant was removed. The bacterial suspensions in sets A1 and A2 were removed from the 4°C fridge and centrifuged at 10,000 rcf and 4°C for 6 minutes. Once the centrifugation was complete, 650 µL of the supernatant was removed. The steps described in this section are illustrated in Figure 4.3.6.1.

4.3.7 Trypan Blue Fluorescence Quenching

As a result of the steps described previously, there were 20 tubes of RAW 264.7 cells, with or without bacteria, and 6 tubes of FITC-labeled *K. pneumoniae*. All the tubes had a total volume of 350 µL. The contents of sets A1, C, E, and G were resuspended with 350 µL of HBSS. The contents in tubes of sets A2, D, F, and H received 350 µL of 360 µg/mL trypan blue (obtained by diluting a 0.4% trypan blue solution with HBSS). Thus, the tubes in sets A2, D, F, and H contained 700 µL of a trypan blue concentration of 180 µg/mL. The tubes in sets A1, C, E, and G contained a final volume of 700 µL.

All tubes were inverted up and down once to ensure that the contents of the tubes were thoroughly mixed. Then, all tubes sat on ice for 15 minutes. Afterwards, the contents of all tubes were centrifuged at 750 rcf and 4°C for 10 minutes. The 20 tubes containing RAW cells were taken out of the centrifuge, and tubes of sets A1 and A2 were left to centrifuge at 10,000 rcf and 4°C for 6 minutes. While the bacteria were centrifuging, 550 µL of the supernatant in tubes of sets C, D, E, F, G, and H was removed. Next, those same tubes received 1 mL of HBSS with 1% HI-FBS. As a result, tubes in sets C, E, and G contained 1.15 mL of 3.5×10^5 cells/mL. Tubes in sets D, F, and H had 1.15 mL of 3.5×10^5 trypan blue quenched cells/mL.

After aliquoting out 1 mL of HBSS with 1% HI-FBS to tubes in sets C through H, tubes in sets A1 and A2 were taken out of the centrifuge. 550 µL of the supernatant from each tube was removed. The tubes in sets A1 and A2 received 1 mL of chilled HBSS with 1% HI-FBS. As a result, tubes in set A1 had 1.15 mL of 4.0×10^7 FITC-labeled bacteria/mL. Tubes in set A2 contained 1.15 mL of 4.0×10^7 FITC-labeled, trypan blue quenched bacteria/mL. The steps described in this section are illustrated in Figure 4.3.7.1.

4.3.8 Fluorescence Plate Reading

Tubes in sets A1, A2, C, D, E, F, G, and H were plated on a 96 well black, clear flat bottom non-treated polystyrene microplate (Corning). Two wells, each with 200 uL, were plated for every tube in sets A1 and A2. Three wells, each with 200 uL, were plated for every individual tube in sets C through H. A bottom reading of the plate was taken with an EnSight Multimode Microplate Reader (PerkinElmer). The steps described in this section are illustrated in Figure 4.3.7.1.

4.3.9 Data Analysis

All data analysis was done in Microsoft Excel. The steps for how the calculations to compare opsonized and non-opsonized, FITC-labeled bacteria are shown in Figure 4.3.9.1. First, the average of the fluorescence intensities of HBSS with 5% HI-FBS were obtained. Next, that average was subtracted from the individual fluorescence values of opsonized and non-opsonized, FITC-labeled bacteria. In doing so, the fluorescence background from HBSS with 5% HI-FBS was removed. Then, the average of the individual adjusted fluorescence intensities corresponding for a sample was calculated. The ratio of fluorescence between opsonized and non-opsonized FITC-labeled bacteria for a given sample was obtained by dividing the average of opsonized FITC-labeled bacteria for a sample by the average of non-opsonized FITC-labeled bacteria for a sample. The overall assessment of the fluorescence difference between opsonized and non-opsonized FITC-labeled bacteria was determined by averaging the values obtained from the previous step.

The steps for the calculations to determine the extent to which trypan blue quenched the fluorescence of FITC-labeled bacteria is illustrated in Figure 4.3.9.2. First, the average of the fluorescence intensities of HBSS with 1% HI-FBS were taken. Next, that average was subtracted

from the individual fluorescence values of FITC-labeled bacterial samples that either were quenched or unquenched with trypan blue. In doing so, the fluorescence background from HBSS with 1% HI-FBS was removed. Then, the average of the individual adjusted fluorescence intensities corresponding for a given sample was calculated. As shown in step 4, the amount of fluorescence remaining after trypan blue quenching was obtained by dividing the average of quenched FITC-labeled bacteria for one sample by the average of unquenched FITC-labeled bacteria for one sample. Step 5 was performed to get a value that represented the degree to which trypan blue quenched FITC-labeled bacteria for a given sample. Step 6 was performed to assess the overall quenching of fluorescence by trypan blue.

The steps for how the calculations to determine extent of phagocytosis, defined as the amount of bacteria phagocytosed, is shown in Figure 4.3.9.3. First, the average of the individual fluorescence values of unquenched RAW cells and quenched RAW cells were obtained. Next, the control averages were subtracted from their respective experimental samples' individual fluorescence intensities. For example, quenched RAW cells with either opsonized or non-opsonized, FITC-labeled bacteria were subtracted by the average of quenched RAW cells. This is shown in step 3 of Figure 4.3.9.3. Next, as shown in step 4, the adjusted fluorescence intensities for quenched and unquenched samples with opsonized or non-opsonized bacteria were averaged. Finally, the extent of phagocytosis for one sample was determined by dividing the average of quenched RAW cells with opsonized or non-opsonized FITC-labeled bacteria for one sample by its unquenched counterpart. For example, the extent of phagocytosis of opsonized bacteria for one sample would be determined by dividing the average fluorescence of quenched RAW cells with opsonized FITC-labeled bacteria by the average fluorescence of unquenched RAW cells with opsonized FITC-labeled bacteria. This is illustrated in step 5 of Figure 4.3.9.3.

4.4 Results

All of the FITC-labeled bacterial samples exhibited higher fluorescence readings than the blank HBSS solutions, indicating that the bacteria were labeled. However, opsonized, FITC-labeled bacteria had a fluorescence that was 25 ± 2% of the non-opsonized, FITC-labeled bacteria.

Trypan blue was able to quench 43.5 ± 0.7% of the fluorescence exhibited by FITC-labeled bacteria.

The average extent of phagocytosis, defined as the amount of bacteria phagocytosed, of non-opsonized bacteria (n = 4) was 59.85% with data points of 51.78%, 37.52%, 97.82%, and 52.26%. The standard deviation for non-opsonized bacteria was 26.23. The average extent of phagocytosis of opsonized bacteria (n = 4) was 46.29% with data points of 58.67%, 26.74%, 25.71%, and 74.05%. The standard deviation for opsonized bacteria was 24.00. The data for opsonized and non-opsonized bacteria is plotted in Figure 4.4.1. It is important to note that sometimes, the calculations described in Figure 4.3.9.3 resulted in an extent of phagocytosis value that was larger than 100% or negative. These values were considered as outliers and not included in determining the overall extent of phagocytosis of opsonized and non-opsonized bacteria. It is not logical to have phagocytosis that exceeds 100% or be negative.

For this experiment, a two-sided t-test was used. The null hypothesis stated that there was no statistical difference in phagocytosis between opsonized and non-opsonized bacteria. The alternative hypothesis stated that there was a difference in phagocytosis between opsonized and non-opsonized bacteria. The calculated t and p values were 0.7623 and 0.4748, respectively, making the results not significant at $p < 0.05$. Thus, there was no indication that the artificial opsonin caused a statistical difference in phagocytosis between opsonized and non-opsonized

bacteria. However, it is possible that the opsonin had an effect, but the effect was not large enough to be considered statistically significant.

4.5 Discussion

4.5.1 Difference in Fluorescence between Opsonized and Non-opsonized Bacteria

The fluorescence intensity difference between opsonized and non-opsonized bacteria can be attributed to the opsonin itself. The non-opsonized and opsonized bacteria underwent the same treatments (same incubation times, bacteria source, labeling conditions, solution etc.) except for their exposure to opsonin. There are two possible explanations for this phenomena: (1) the artificial opsonin is displacing FITC, and (2) the artificial opsonin is pulling FITC off the gram-negative bacteria. In the first explanation, the artificial opsonin was designed to bind to LPS. It is possible that the artificial opsonin's designed affinity to LPS of gram-negative bacteria could displace FITC off of the bacterial membrane. FITC has been conjugated to LPS in experiments, suggesting that FITC binds to LPS to fluorescently label LPS [55]. Based on Bhunia et al. [17] proposed model of how YI12WF binds to LPS, YI13WF could be binding to LPS and disrupting the LPS structure. As a result, FITC could be displaced from LPS. Nevertheless, a wash designed to remove excess opsonin could also remove FITC as well.

In the second explanation, excess artificial opsonin that doesn't bind to FITC-labeled *K. pneumoniae* is able to remove FITC off of the bacteria. It is known that FITC binds to primary amines and the N-terminus of a peptide [56]. The artificial opsonin contains arginine and lysine, amino acids that have primary amines as their side chains. These amino acids are located in di-tuftsin and YI13WF. As a result, the two components of the artificial opsonin provide potential binding sites for FITC. Thus, a wash designed to remove excess opsonin could also remove opsonin-FITC complexes.

In both explanations, the thiourea bond formed when FITC binds to primary amines must be broken. However, this bond is stable, and it would be difficult to break the thiourea bond.

In order to determine which explanation is true, the dissociation constant (K_d) of bacteria with opsonin and relative bond strengths between two complexes, FITC with bacteria and FITC with opsonin, would need to be found. Knowing the relative strengths of the bonds found in each complex and the K_d of bacteria with opsonin would elucidate on the likelihood that the complexes would break into its individual components or remain intact.

4.5.2 FITC Quenching of Bacteria

As stated previously, only 43.5 ± 0.7% of the fluorescence exhibited by FITC-labeled bacteria was quenched by trypan blue. Although this may seem insufficient, it is adequate. The bacterial samples used to determine the extent of quenching by trypan blue contained 4.6×10^7 bacteria, while 8.0×10^6 bacteria were used to mix with the RAW cells. Thus, the controls had 5.75 times the number of bacteria used for the phagocytosis assay. If 43.5% of the controls experienced FITC quenching, that would mean that 2.0×10^7 bacteria, or 2.5 times the amount of bacteria used in the phagocytosis assay, would have been quenched. Thus, it can be assumed that the fluorescence from FITC-labeled bacteria adhering to the exterior of macrophages during the phagocytosis assay was thoroughly quenched.

4.5.3 Factors in determining the Extent of Phagocytosis

One factor that could affect phagocytosis is the capability to stop it. All the tubes, whether containing RAW 264.7 cells or bacteria, were kept on ice after phagocytosis had occurred. In addition, the centrifuge was set to 4°C. Theoretically, placing the tubes on ice should stop phagocytosis. However, it is possible that the temperature settings and the placement of tubes on ice were not enough to stop phagocytosis. In order to ensure the stoppage of phagocytosis,

cytochalasin D can be used. Cytochalasin D inhibits actin polymerization, which can block phagocytosis [57].

Based on the assay and the calculations performed to determine extent of phagocytosis, it is imperative to have bacteria that is as bright as possible. The difference in fluorescence between opsonized and non-opsonized FITC-labeled bacteria has an impact on the calculations. The fluorescence intensities of experimental samples containing quenched or unquenched RAW 264.7 cells, with either opsonized or non-opsonized FITC-labeled bacteria, must exceed the fluorescence intensities of controls containing only quenched or unquenched RAW 264.7 cells. If the fluorescence intensities between the experimental samples and controls are too numerically close, which happened in this assay, then it is hard to differentiate between the two groups. As a result, the adjusted fluorescence intensities of quenched RAW 264.7 cells with opsonized or non-opsonized bacteria, obtained in step 3 of Figure 4.3.9.3, can be negative or larger than the fluorescence intensities of unquenched RAW 264.7 cells with opsonized or non-opsonized bacteria, respectively.

To compound the issue, it is important to have a distinction in fluorescence between quenched and unquenched RAW 264.7 cells with either opsonized or non-opsonized bacteria. As seen in step 5 of Figure 4.3.9.3, the unquenched sample must have a larger fluorescence value than the quenched sample. Otherwise, it can also lead to phagocytosis determinations of negative percentages or percentages greater than 100%.

On average, quenched RAW 264.7 cells with either opsonized or non-opsonized FITC-labeled bacteria had lower fluorescence intensities than unquenched RAW 264.7 cells with either opsonized or non-opsonized FITC-labeled bacteria. However, as shown in step 5 of Figure 4.3.9.3, the extent of phagocytosis is determined when comparing between individual

experimental samples; the average plays no role in the final outcome when determining the amount of bacteria phagocytosed.

It would have been ideal for the bacteria, opsonized or not, to have the same fluorescence. In order to improve this assay, the bacteria, with or without opsonin, must be washed after incubation for an hour. In doing so, it would hopefully reduce the difference in fluorescence between the two groups.

Another crucial component in determining the extent of phagocytosis is the amount of trypan blue that is not washed away. As already discussed in the introduction of this chapter, trypan blue can quench FITC fluorescence. The amount of trypan blue remaining correlates to the strength of the FITC signal that can be read. Using excessive amounts of trypan blue can prevent the FITC-labeled bacteria from exerting fluorescence, which would make the quenched and unquenched RAW 264.7 control samples indistinguishable from the experimental samples containing quenched and unquenched RAW 264.7 cells with FITC-labeled bacteria. In addition, trypan blue at high concentrations is toxic to cells [58-59]. According to Chan et al. [59], when cells are mixed with trypan blue, trypan blue adds negatively charged residues on the cell's cytoplasm. The negative charges attract positive ions, which induces an influx of water into the cells that could potentially make the cells burst [59]. On the other hand, minute quantities of trypan blue would not eliminate all the fluorescence from the extracellular bacteria not phagocytosed, making it difficult to differentiate between fluorescent bacteria adhering to the exterior of macrophages and phagocytosed, fluorescent bacteria residing inside the macrophages. As a result, a certain amount of trypan blue, optimized to the user, needs to be utilized.

4.5.4 Alternative Methods for Phagocytosis Assay

In this assay, a plate reader was used to determine the extent of phagocytosis. However, in many phagocytosis assays, a flow cytometer is used [52-54]. A flow cytometer is superior to a plate reader because a flow cytometer captures a certain number of cells dictated by the user. With a plate reader, the differences in pipetting can lead to different amounts of bacteria and cells present in the well and, ultimately, variations in fluorescence outputs; a flow cytometer avoids these issues. As a result, a flow cytometer is more precise in capturing data than a plate reader when the samples have trypan blue.

The downside of using a flow cytometer is that it is much more complex. Compensation controls are needed if two or more colors are detected with the flow cytometer. In addition, the analysis utilizing FlowJo may be confusing and is prone to human bias since the user forms gates to select on certain populations of cells.

As discussed in section 4.5.3, quenching with trypan blue has a substantial impact on how this phagocytosis assay works. In order to avoid using trypan blue, bacteria expressing green fluorescent protein (GFP) can be used in phagocytosis assays [60-61]. GFP-expressing bacteria dodges the necessity to FITC label bacteria and does not succumb to the sensitive nature of trypan blue. In order to differentiate between extracellular and intracellular bacteria, the macrophages would need to be stained with or express a different fluorescence color than GFP. The macrophages and bacteria would be mixed and cytochalasin D would be added to stop phagocytosis. Afterwards, the samples would be run through a flow cytometer. FlowJo could be used to analyze the results and determine the extent of phagocytosis of opsonized and non-opsonized bacteria.

4.6 Conclusion

The artificial opsonin did not cause a statistical significance in phagocytosis of FITC-labeled *K. pneumoniae* by RAW 264.7 cells. However, this does not signify that the artificial opsonin did not elicit any difference whatsoever; the impact may be too small to be detected. There were many factors that affected the end result, and it's plausible that tinkering with these variables may change the outcome. While a sufficient amount of trypan blue was used to quench extracellular FITC-labeled bacteria, trypan blue had a profound impact on the plate reading due to trypan blue's strong quenching capabilities and toxicity to cells. Besides that, the opsonized bacteria exhibited lower fluorescence than the non-opsonized bacteria. Considering that fluorescence intensities of the controls and the experimental samples in the phagocytosis assay were numerically close to one another, the difference in fluorescence between the two types of bacteria can make a difference. Based on the fact that the phagocytosis assay performed could be optimized or even be replaced with a different phagocytosis assay, as indicated in section 4.5.4, the artificial opsonin's effect on phagocytosis is inconclusive. However, for the time being, it can be said that the bacteria opsonized with the artificial opsonin does not statistically significantly increase or decrease phagocytosis.

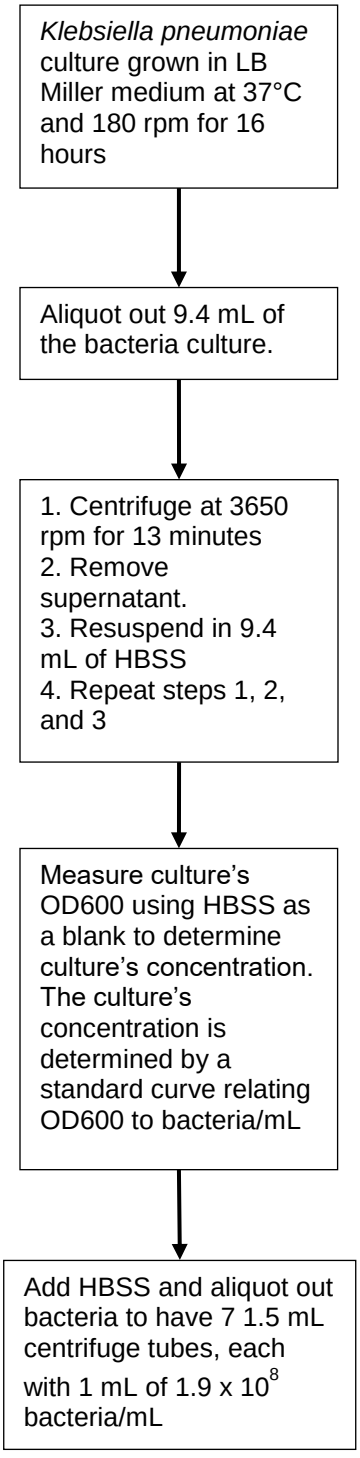

Figure 4.3.1.1: A flowchart describing how the *K. pneumoniae* bacteria culture was prepared for FITC labeling

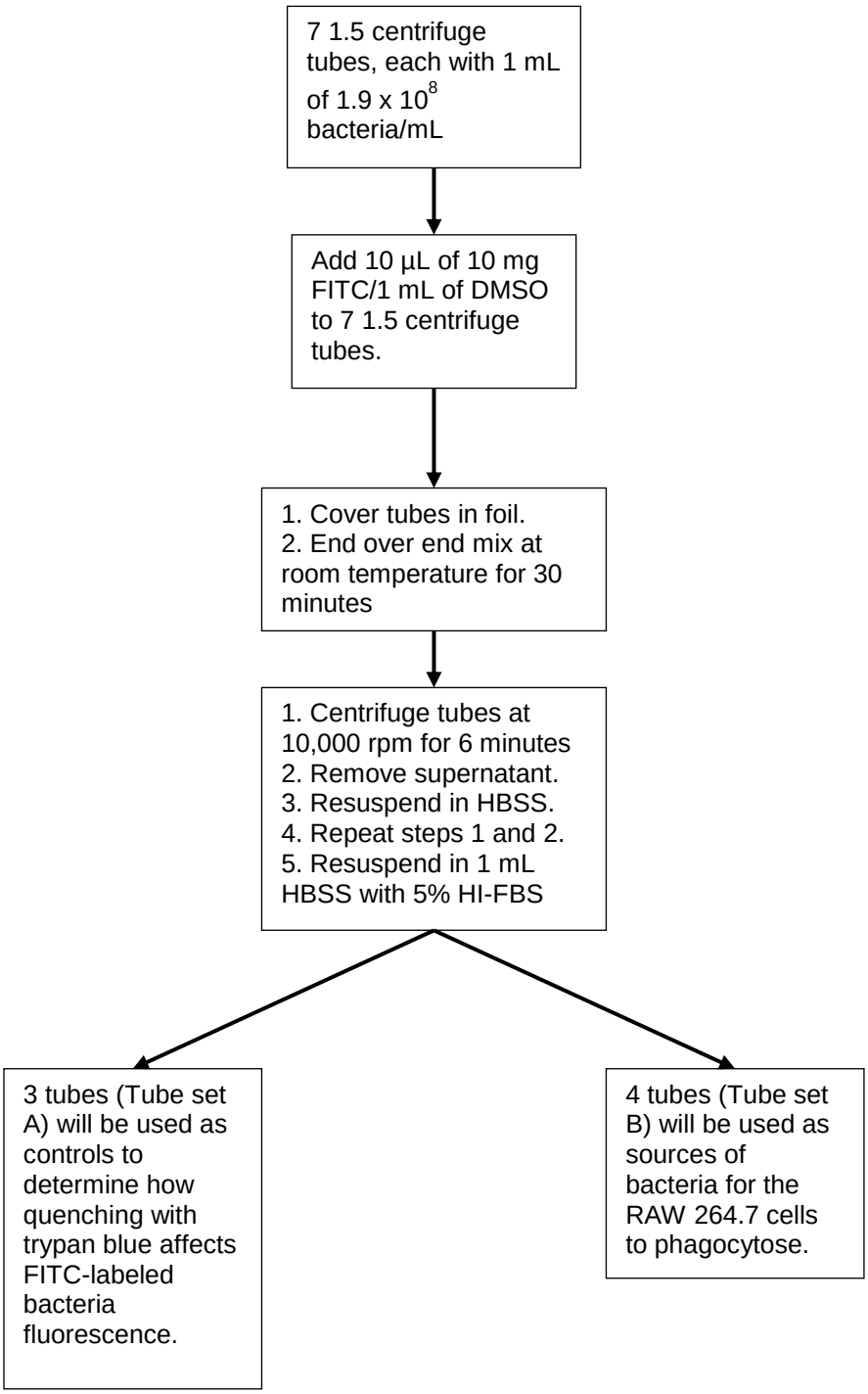

Figure 4.3.2.1: A flowchart describing how the *K. pneumoniae* bacteria was FITC-labeled

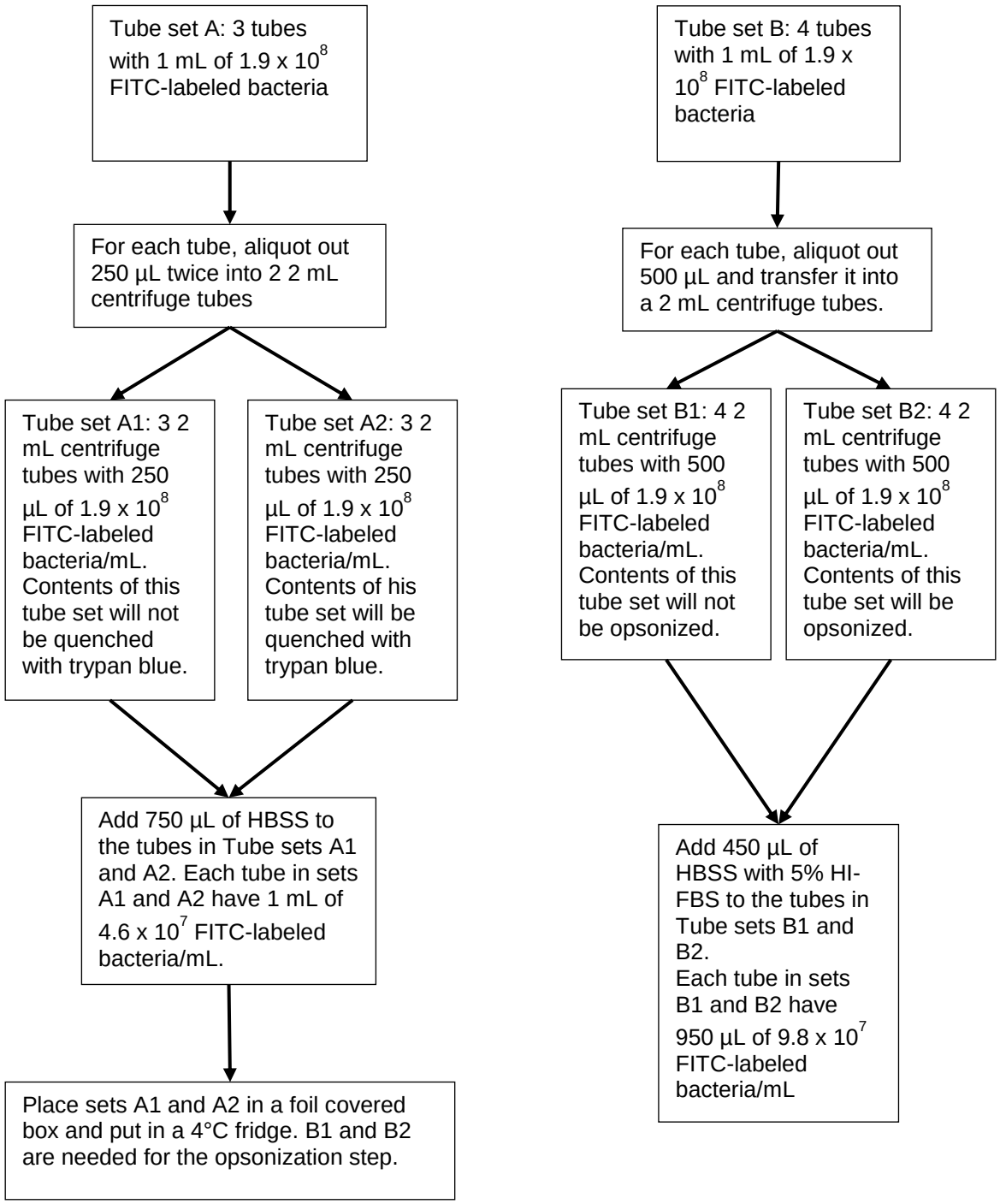

Figure 4.3.3.1: A flowchart describing how FITC-labeled *K. pneumoniae* was prepared for opsonization or for future steps in the phagocytosis assay

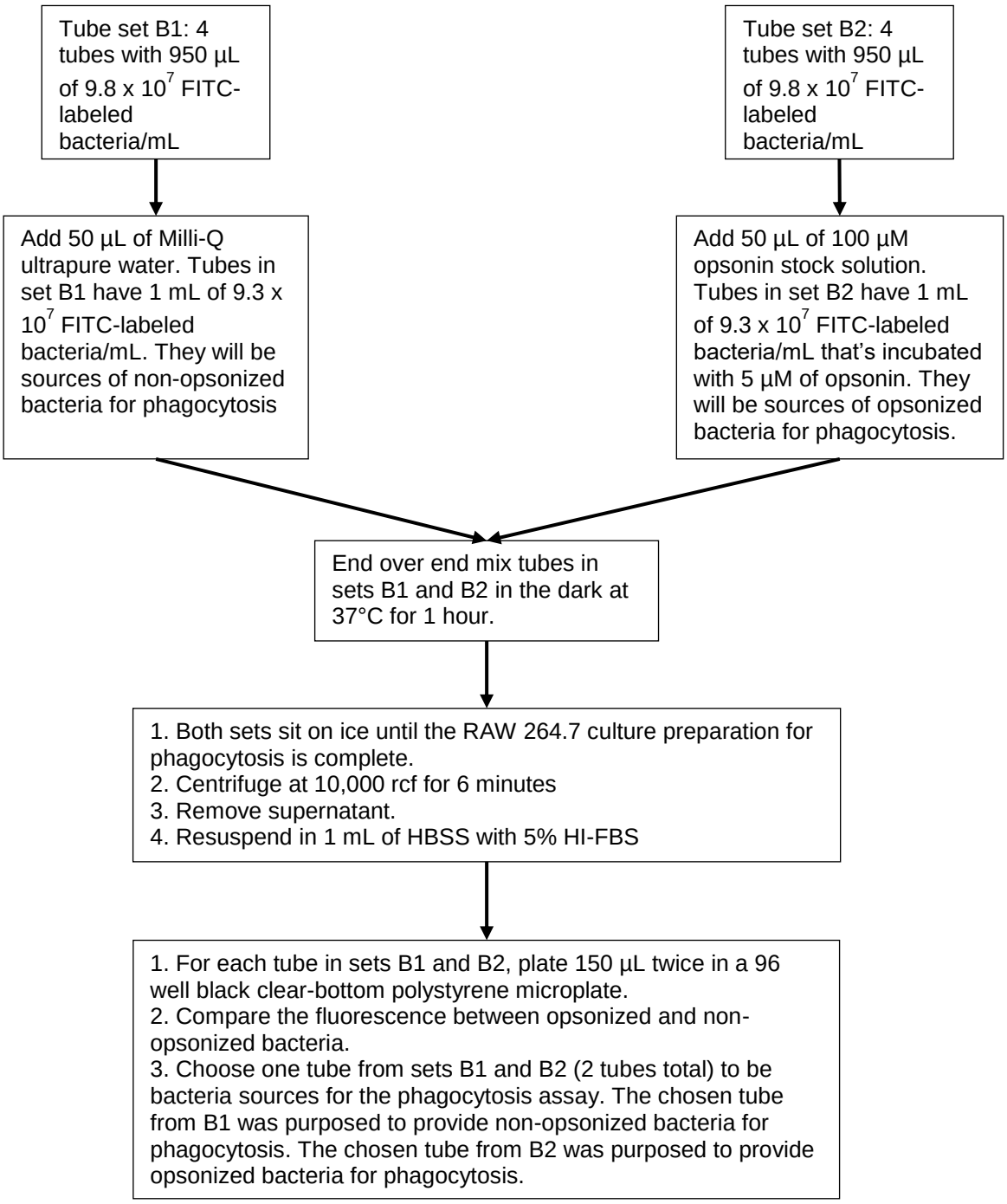

Figure 4.3.4.1: A flowchart describing how FITC-labeled *K. pneumoniae* bacteria was opsonized

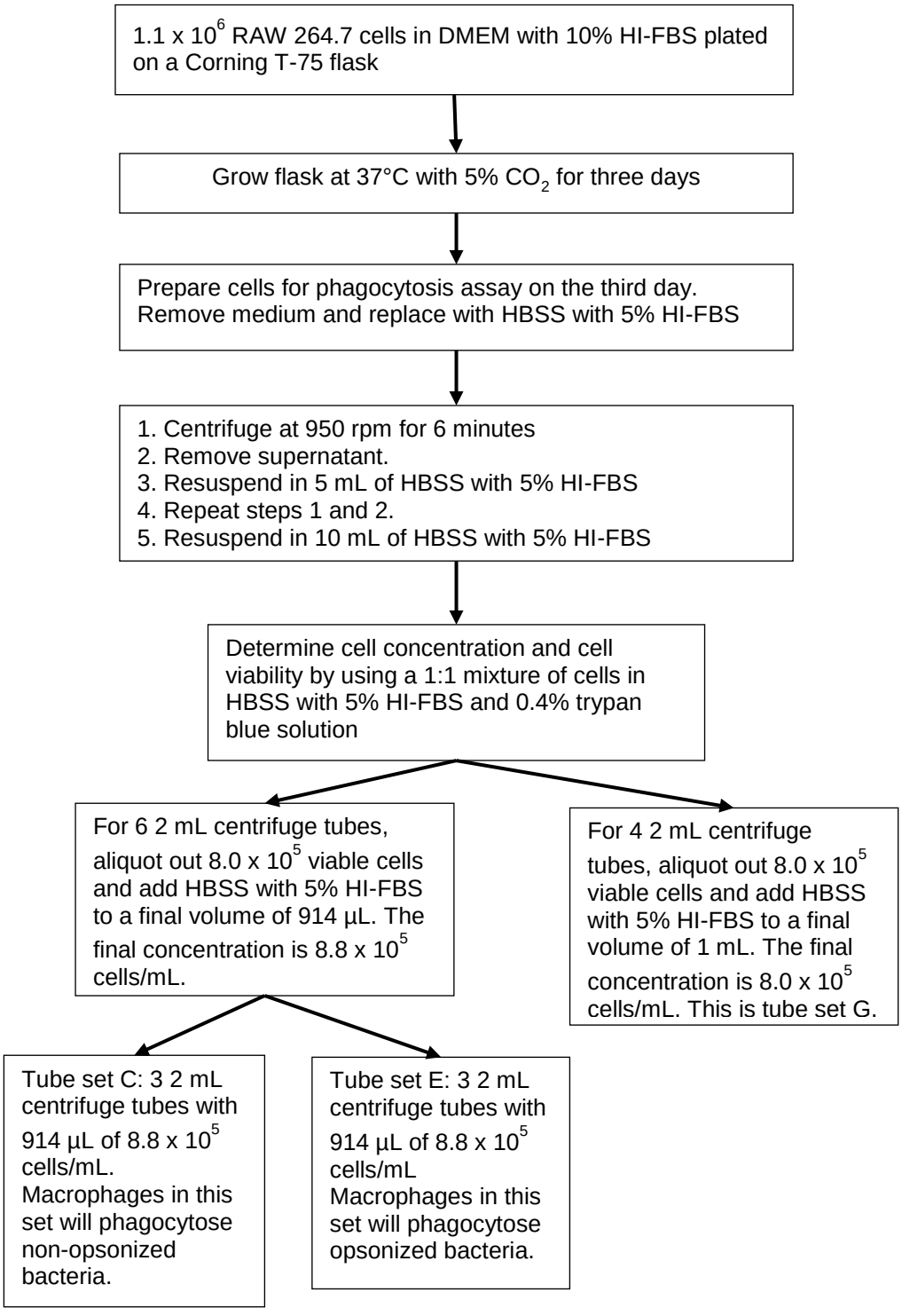

Figure 4.3.5.1: A flowchart describing how the RAW 264.7 culture was prepared for the phagocytosis assay

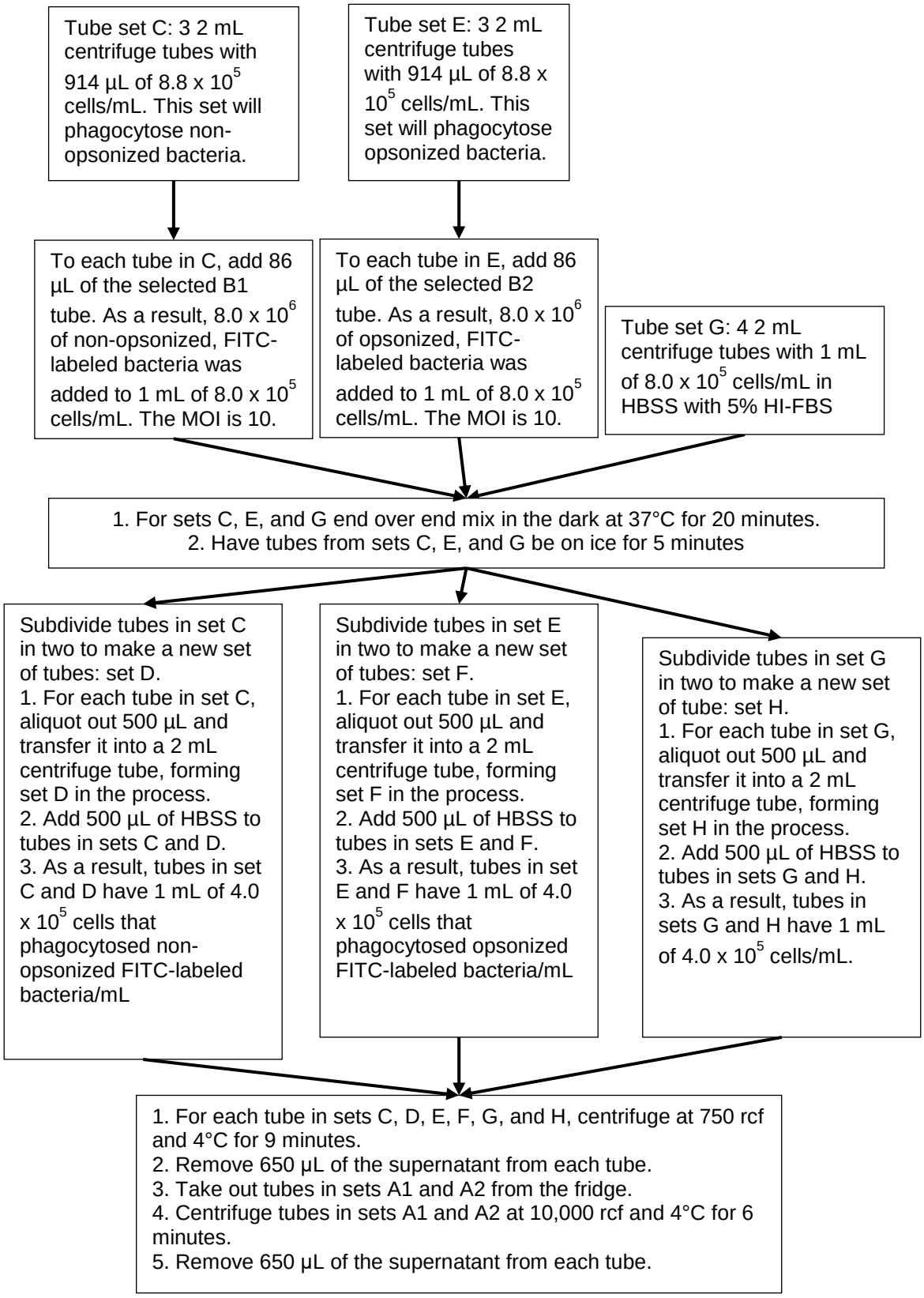

Figure 4.3.6.1: A flowchart describing the procedure of how RAW 264.7 phagocytosed non-opsonized and opsonized *K. pneumoniae*

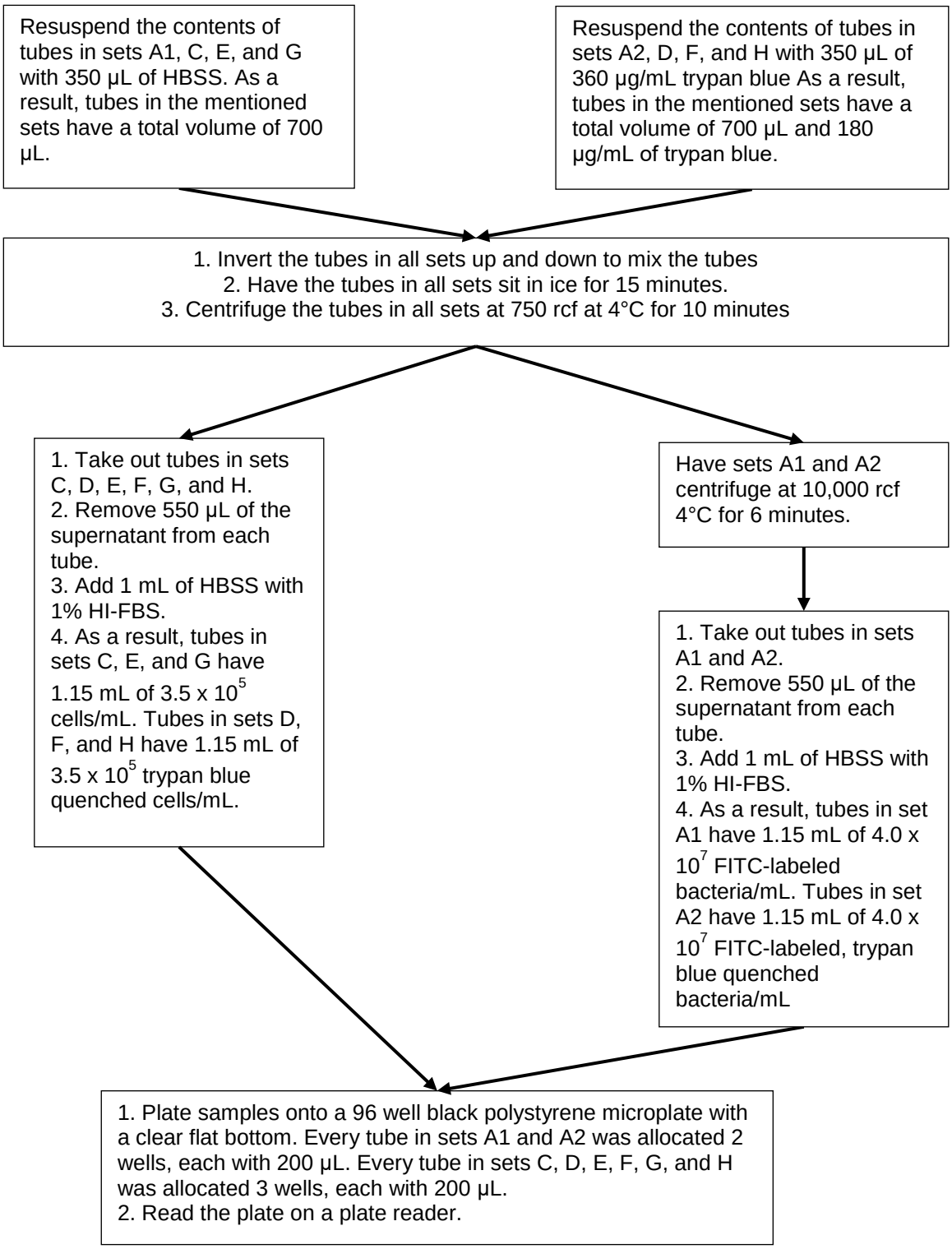

Figure 4.3.7.1: A flowchart describing the procedure of trypan blue quenching and plating of the samples onto a 96 well black polystyrene microplate with a clear flat bottom.

B1a, B1b = individual fluorescence intensities for one sample of non-opsonized FITC-labeled bacteria

B2a, B2b = individual fluorescence intensities for one sample of opsonized FITC-labeled bacteria

Y1, Y2, Y3, Y4 = individual fluorescence intensities of HBSS with 5% HI-FBS

Step 1: Average Y1, Y2, Y3, and Y4 = AY (average of Y)

Step 2: Subtract average of HBSS with 5% HI-FBS from individual fluorescence intensities of samples

[Bla – AY], [B1b – AY]

[B2a – AY], [B2b – AY]

Step 3: Average the values obtained from Step 2

Average of [Bla – AY], [B1b – AY] = AB1 (average of one sample of B1)

Average of [B2a – AY], [B2b – AY] = AB2 (average of one sample of B2)

Step 4: Use the following formula

[ratio of fluorescence between opsonized and non-opsonized FITC-labeled bacteria] =

$$\frac{[\text{average fluorescence of opsonized FITC-labeled bacteria for one sample}]}{[\text{average fluorescence of non-ospsonized FITC-labeled bacteria for one sample}]} = \frac{[AB2]}{[AB1]}$$

Step 5: Average the values obtained from step 4 to determine the overall ratio of fluorescence between opsonized and non-opsonized FITC-labeled bacteria.

Figure 4.3.9.1: Description of how the calculations to compare the fluorescence between opsonized and non-opsonized FITC-labeled bacteria for one sample. There were four samples of opsonized and non-opsonized FITC-labeled bacteria per phagocytosis experiment.

A1a, A1b = individual fluorescence intensities for one sample of unquenched (no trypan blue) FITC-labeled bacteria

A2a, A2b = individual fluorescence intensities for one sample of for trypan blue quenched FITC-labeled bacteria

X1, X2, X3, X4 = individual fluorescence intensities of HBSS with 1% HI-FBS

Step 1: Average X1, X2, X3, and X4 = AX (average of X)

Step 2: Subtract average of HBSS with 1% HI-FBS from individual fluorescence intensities of samples

[Ala – AX], [A1b – AX]

[A2a – AX], [A2b – AX]

Step 3: Average the values obtained from Step 2

Average of [Ala – AX], [A1b – AX], = AA1 (average of one sample of A1)

Average of [A2a – AX], [A2b – AX] = AA2 (average of one sample of A2)

Step 4: Use the following formula

[amount of fluorescence that remains after quenching with trypan blue] =

$$\frac{[\text{average fluorescence of quenched FITC-labeled bacteria for one sample}]}{[\text{average fluorescence of unquenched FITC-labeled bacteria for one sample}]} = \frac{[AA2]}{[AA1]}$$

Step 5: Use the following formula

[extent to which trypan blue quenched FITC-labeled bacteria] =

$$1 - \left(\frac{[\text{average fluorescence of quenched FITC-labeled bacteria for one sample}]}{[\text{average fluorescence of unquenched FITC-labeled bacteria for one sample}]}\right) = 1 - \frac{[AA2]}{[AA1]}$$

Step 6: Average the values obtained from step 5 to determine the overall quenching capability of trypan blue on FITC-labeled bacteria for a specific experiment.

Figure 4.3.9.2: Description of how the calculations to determine the extent of FITC quenching by trypan blue for one sample in a phagocytosis experiment. There were two samples each of quenched and unquenched FITC-labeled bacteria per phagocytosis experiment.

C1, C2, C3 = individual fluorescence intensities for unquenched RAW cells with non-opsonized, FITC-labeled bacteria of one sample

D1, D2, D3 = individual fluorescence intensities for quenched RAW cells with non-opsonized, FITC-labeled bacteria of one sample

E1, E2, E3 = individual fluorescence intensities for unquenched RAW cells with opsonized, FITC-labeled bacteria of one sample

F1, F2, F3 = individual fluorescence intensities for quenched RAW cells with opsonized, FITC-labeled bacteria of one sample

G1, G2, G3, G4 = individual fluorescence intensities for unquenched RAW cells of one sample

H1, H2, H3, H4 = individual fluorescence intensities for quenched RAW cells of one sample

Step 1: Average G1, G2, G3, and G4 = AG (average of G)

Step 2: Average of H1, H2 H3, and H4 = AH (average of H)

Step 3: Subtract individual fluorescence intensities by their respective controls. The control for C1 through C3 and E1 through E3 is unquenched RAW cells. The control for D1 through D3 and F1 through F3 is quenched RAW cells.

[C1 – AG], [C2 – AG], [C3 – AG]

[D1 – AH], [D2 – AH], [D3 – AH]

[E1 – AG], [E2 – AG], [E3 – AG]

[F1 – AH], [F2 – AH], [F3 – AH]

Step 4: Average the values obtained from Step 3

Average of [C1 – AG], [C2 – AG], [C3 – AG] = AC (average of one sample of C)

Average of [D1 – AH], [D2 – AH], [D3 – AH] = AD (average of one sample of D)

Average of [E1 – AG], [E2 – AG], [E3 – AG] = AE (average of one sample of E)

Average of [F1 – AH], [F2 – AH], [F3 – AH] = AF (average of one sample of F)

Step 5: Use the following formula

[extent of phagocytosis for opsonized or non-opsonized bacteria] =

$$\frac{[\text{average of quenched RAW cells with opsonized or non} - \text{opsonized FITC} - \text{labeled bacteria for one sample}]}{[\text{average of unquenched RAW cells with opsonized or non} - \text{opsonized FITC} - \text{labeled bacteria for one sample}]}$$

[extent of phagocytosis of opsonized bacteria from one sample] = $\frac{[\text{AF}]}{[\text{AE}]}$

[extent of phagocytosis of non-opsonized bacteria from one sample] = $\frac{[\text{AD}]}{[\text{AC}]}$

Figure 4.3.9.3: Description of how the calculations to determine the extent of phagocytosis were done for one sample in one phagocytosis experiment. Each phagocytosis experiment included 3 samples of groups C, D, E, and F. Each experiment included 4 samples of G and H. The calculations were done for each sample in a phagocytosis experiment.

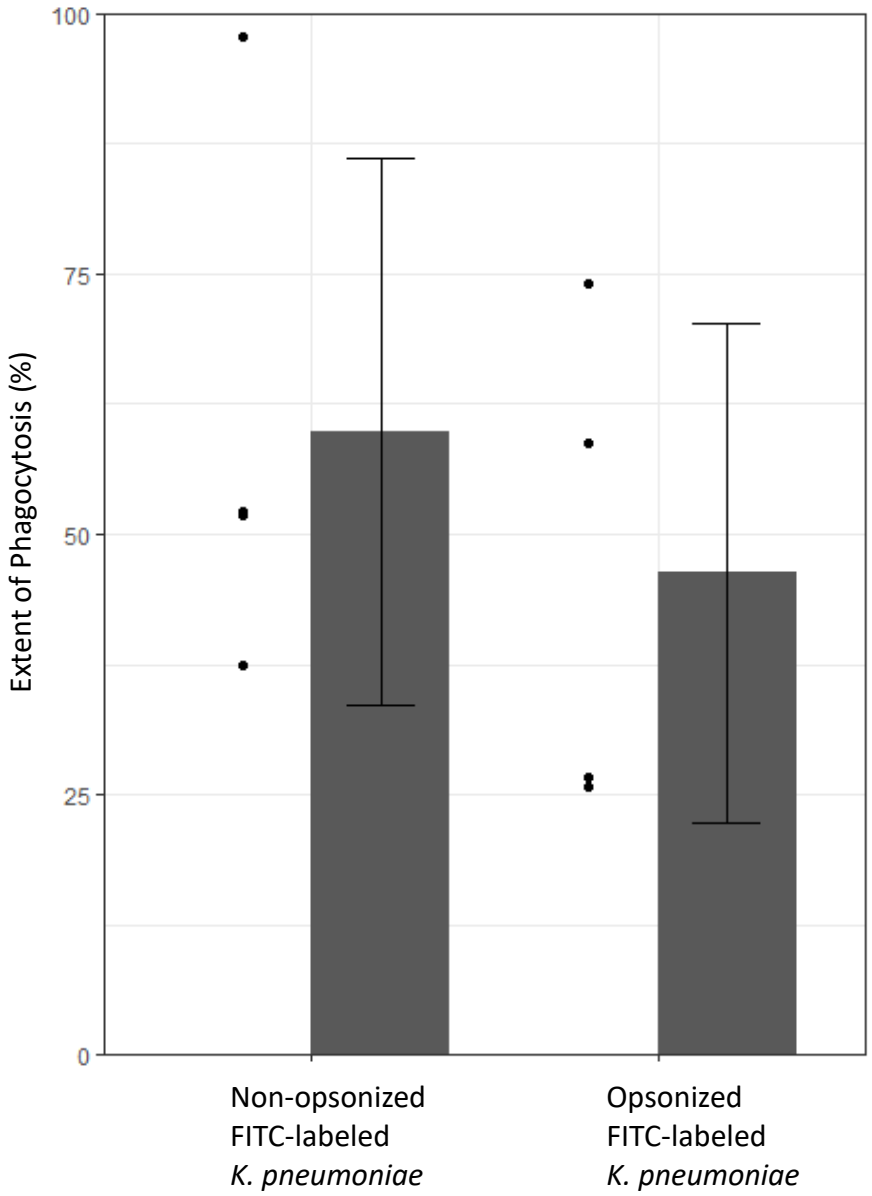

Figure 4.4.1: Bar and scatter plot detailing the extent of phagocytosis of non-opsonized and opsonized FITC-labeled *K. pneumoniae*. The scatter plot represents the individual data points for each group (n = 4), and the bar represents the average of those data points. The error bars represent one standard deviation above and below the average.

Chapter 5: Overall Conclusions

A multivalent artificial opsonin to target and phagocytose gram-negative bacteria was evaluated. The artificial opsonin showed affinity to both gram-positive and gram-negative bacteria. In addition, using more opsonin increased the degree to which the bacteria were opsonized. The opsonin showed that it could bind to RAW 264.7 mouse macrophages. Again, incubating the RAW 264.7 cells with more opsonin increased the extent to which the cells were saturated. Lastly, the difference in phagocytosis of non-opsonized and opsonized *Klebsiella pneumoniae* was not statistically significant, but that does not exclude the possibility that the opsonin had an effect. Several imperative factors had an impact on the end result that could possibly sway the outcome. However, as of now, the artificial opsonin does not lead to a statistically significant increase in phagocytosis.

Literature Citations

[1] Peleg, A. Y., & Hooper, D. C. (2010). Hospital-acquired infections due to gram-negative bacteria. *The New England journal of medicine*, *362*(19), 1804–1813. https://doi.org/10.1056/NEJMra0904124

[2] Haque, M., Sartelli, M., McKimm, J., & Abu Bakar, M. (2018). Health care-associated infections - an overview. *Infection and drug resistance*, *11*, 2321–2333. https://doi.org/10.2147/IDR.S177247

[3] Khan, H. A., Ahmad, A., & Mehboob, R. (2015). Nosocomial infections and their control strategies. *Asian Pacific Journal of Tropical Biomedicine*, *5*(7), 509–514. https://doi.org/10.1016/j.apjtb.2015.05.001

[4] Ashurst, J. V., & Dawson, A. (2020). Klebsiella Pneumonia. In *StatPearls*. StatPearls Publishing. http://www.ncbi.nlm.nih.gov/books/NBK519004/

[5] Struve, C., & Krogfelt, K. A. (2004). Pathogenic potential of environmental Klebsiella pneumoniae isolates. *Environmental Microbiology*, *6*(6), 584–590. https://doi.org/10.1111/j.1462-2920.2004.00590.x

[6] Seifi, K., Kazemian, H., Heidari, H., Rezagholizadeh, F., Saee, Y., Shirvani, F., & Houri, H. (2016). Evaluation of Biofilm Formation Among Klebsiella pneumoniae Isolates and Molecular Characterization by ERIC-PCR. *Jundishapur journal of microbiology*, *9*(1), e30682. https://doi.org/10.5812/jjm.30682

[7] Stone P. W. (2009). Economic burden of healthcare-associated infections: an American perspective. *Expert review of pharmacoeconomics & outcomes research*, *9*(5), 417–422. https://doi.org/10.1586/erp.09.53

[8] Centers for Disease Control and Prevention. (2019, August 8). Antibiotic Use in Hospitals, 2017. https://www.cdc.gov/antibiotic-use/stewardship-report/hospital.html

[9] Centers for Disease Control and Prevention. (2020, February 10). How Antibiotic Resistance Happens. https://www.cdc.gov/drugresistance/about/how-resistance-happens.html

[10] Collins, A. S. (2008). Preventing Health Care–Associated Infections. In R. G. Hughes (Ed.), *Patient Safety and Quality: An Evidence-Based Handbook for Nurses*. Agency for Healthcare Research and Quality (US). http://www.ncbi.nlm.nih.gov/books/NBK2683/

[11] Jacobsen, S. M., Stickler, D. J., Mobley, H. L., & Shirtliff, M. E. (2008). Complicated catheter-associated urinary tract infections due to Escherichia coli and Proteus mirabilis. *Clinical microbiology reviews*, *21*(1), 26–59. https://doi.org/10.1128/CMR.00019-07

[12] Jacobsen, S. M., Stickler, D. J., Mobley, H. L., & Shirtliff, M. E. (2008). Complicated catheter-associated urinary tract infections due to Escherichia coli and Proteus mirabilis. *Clinical microbiology reviews*, *21*(1), 26–59. https://doi.org/10.1128/CMR.00019-07

[13] Rimondini, L., Fini, M., & Giardino, R. (2005). The Microbial Infection of Biomaterials: A Challenge for Clinicians and Researchers. A Short Review. *Journal of Applied Biomaterials and Biomechanics*, *3*(1), 1–10. https://doi.org/10.1177/228080000500300101

[14] Kostakioti, M., Hadjifrangiskou, M., & Hultgren, S. J. (2013). Bacterial biofilms: development, dispersal, and therapeutic strategies in the dawn of the postantibiotic era. *Cold Spring Harbor perspectives in medicine*, *3*(4), a010306. https://doi.org/10.1101/cshperspect.a010306

[15] Hotchkiss, R. S., Moldawer, L. L., Opal, S. M., Reinhart, K., Turnbull, I. R., & Vincent, J. L. (2016). Sepsis and septic shock. *Nature reviews. Disease primers*, *2*, 16045. https://doi.org/10.1038/nrdp.2016.45

[16] Rosenfeld, Y., & Shai, Y. (2006). Lipopolysaccharide (Endotoxin)-host defense antibacterial peptides interactions: Role in bacterial resistance and prevention of sepsis. *Biochimica et Biophysica Acta (BBA) - Biomembranes*, *1758*(9), 1513–1522. https://doi.org/10.1016/j.bbamem.2006.05.017

[17] Bhunia, A., Mohanram, H., Domadia, P. N., Torres, J., & Bhattacharjya, S. (2009). Designed beta-boomerang antiendotoxic and antimicrobial peptides: structures and activities in lipopolysaccharide. *The Journal of biological chemistry*, *284*(33), 21991–22004. https://doi.org/10.1074/jbc.M109.013573

[18] Yu, W.-L., & Chuang , Y.-C. (2019, April 18). Clinical features, diagnosis, and treatment of *Klebsiella pneumoniae* infection. https://www.uptodate.com/contents/clinical-features-diagnosis-and-treatment-of-klebsiella-pneumoniae-infection

[19] Centers for Disease Control and Prevention. (2010, November 24). Klebsiella pneumoniae in Healthcare Settings. https://www.cdc.gov/hai/organisms/klebsiella/klebsiella.html

[20] Prame Kumar, K., Nicholls, A. J., & Wong, C. (2018). Partners in crime: neutrophils and monocytes/macrophages in inflammation and disease. *Cell and tissue research*, *371*(3), 551–565. https://doi.org/10.1007/s00441-017-2753-2

[21] Carrillo, J. L. M., García, F. P. C., Coronado, O. G., García, M. A. M., & Cordero, J. F. C. (2017). Physiology and Pathology of Innate Immune Response Against Pathogens. *Physiology and Pathology of Immunology*. https://doi.org/10.5772/intechopen.70556

[22] Thau, L., & Mahajan, K. (2020). Physiology, Opsonization. In *StatPearls*. StatPearls Publishing. http://www.ncbi.nlm.nih.gov/books/NBK534215/

[23] Hiemstra, P. S., & Daha, M. R. (1998). Opsonization. In P. J. Delves (Ed.), *Encyclopedia of Immunology (Second Edition)* (pp. 1885–1888). Elsevier. https://doi.org/10.1006/rwei.1999.0475

[24] Charles A Janeway, J., Travers, P., Walport, M., & Shlomchik, M. J. (2001). The complement system and innate immunity. *Immunobiology: The Immune System in Health and Disease. 5th Edition*. https://www.ncbi.nlm.nih.gov/books/NBK27100/

[25] Aderem, A., & Underhill, D. M. (1999). Mechanisms of Phagocytosis in Macrophages. *Annual Review of Immunology*, *17*(1), 593–623. https://doi.org/10.1146/annurev.immunol.17.1.593

[26] Rosales, C., & Uribe-Querol, E. (2017). Phagocytosis: A Fundamental Process in Immunity. *BioMed research international*, *2017*, 9042851. https://doi.org/10.1155/2017/9042851

[27] Liu, F., Soh Yan Ni, A., Lim, Y., Mohanram, H., Bhattacharjya, S., & Xing, B. (2012). Lipopolysaccharide Neutralizing Peptide–Porphyrin Conjugates for Effective Photoinactivation and Intracellular Imaging of Gram-Negative Bacteria Strains. *Bioconjugate Chemistry*, *23*(8), 1639–1647. https://doi.org/10.1021/bc300203d

[28] Bhattacharjya, S., Domadia, P. N., Bhunia, A., Malladi, S., & David, S. A. (2007). High-Resolution Solution Structure of a Designed Peptide Bound to Lipopolysaccharide: Transferred Nuclear Overhauser Effects, Micelle Selectivity, and Anti-Endotoxic Activity. *Biochemistry*, *46*(20), 5864–5874. https://doi.org/10.1021/bi6025159

[29] Najjar, V. A. (1988). Tuftsin. In A. J. Sbarra & R. R. Strauss (Eds.), *The Respiratory Burst and Its Physiological Significance* (pp. 449–466). Springer US. https://doi.org/10.1007/978-1-4684-5496-3_22

[30] National Library of Medicine. (2011, November 9). Tuftsin. https://pubchem.ncbi.nlm.nih.gov/compound/53477795

[31] Cammack, R. C., Atwood, T. A., Campbell, P. C., Parish, H. P., Smith, A. S., Vella, F. V., & Stirling, J. S. (2006). Leukokinin. In *Oxford Dictionary of Biochemistry and Molecular Biology*. Oxford University Press. https://www.oxfordreference.com/view/10.1093/acref/9780198529170.001.0001/acref-9780198529170-e-11155

[32] Dagan, S., Gottlieb , P., Fridkin, M., Spirer, Z., Tzehoval , E., & Feldman , M. (1986). The Tuftsin Receptors. In *The Receptors* (Vol. 3, pp. 243–280). Orlando, FL: Academic Press, Inc.

[33] Gupta, C. M., & Haq, W. (2005). Tuftsin-Bearing Liposomes as Antibiotic Carriers in Treatment of Macrophage Infections. In *Methods in Enzymology* (Vol. 391, pp. 291–304). Academic Press. https://doi.org/10.1016/S0076-6879(05)91016-1

[34] Khan, A., Khan, A. A., Dwivedi, V., Ahmad, M. G., Hakeem, S., & Owais, M. (2007). Tuftsin augments antitumor efficacy of liposomized etoposide against fibrosarcoma in Swiss albino mice. *Molecular medicine (Cambridge, Mass.)*, *13*(5-6), 266–276. https://doi.org/10.2119/2007–00018.Khan

[35] Liu, W.-J., Liu, X.-J., Li, L., Li, Y., Zhang, S.-H., & Zhen, Y.-S. (2014). Tuftsin-based, EGFR-targeting fusion protein and its enediyne-energized analog show high antitumor efficacy associated with CD47 down-regulation. *Cancer Immunology, Immunotherapy*, *63*(12), 1261–1272. https://doi.org/10.1007/s00262-014-1604-1

[36] Gottlieb, P., Hazum, E., Tzeboval, E., Feldman, M., Segal, S., & Fridkin, M. (1984). Receptor-mediated endocytosis of tuftsin by macrophage cells. *Biochemical and Biophysical Research Communications*, *119*(1), 203–211. https://doi.org/10.1016/0006-291X(84)91639-5

[37] Wronski, M. A. von, Raju, N., Pillai, R., Bogdan, N. J., Marinelli, E. R., Nanjappan, P., Ramalingam, K., Arunachalam, T., Eaton, S., Linder, K. E., Yan, F., Pochon, S., Tweedle, M. F., & Nunn, A. D. (2006). Tuftsin Binds Neuropilin-1 through a Sequence Similar to That Encoded by Exon 8 of Vascular Endothelial Growth Factor. *Journal of Biological Chemistry*, *281*(9), 5702–5710. https://doi.org/10.1074/jbc.M511941200

[38] Nissen, J. C., Selwood, D. L., & Tsirka, S. E. (2013). Tuftsin signals through its receptor neuropilin-1 via the transforming growth factor beta pathway. *Journal of neurochemistry*, *127*(3), 394–402. https://doi.org/10.1111/jnc.12404

[39] Kuhn, S. E., Nardin, A., Klebba, P. E., & Taylor, R. P. (1998). Escherichia coli Bound to the Primate Erythrocyte Complement Receptor via Bispecific Monoclonal Antibodies Are Transferred to and Phagocytosed by Human Monocytes in an In Vitro Model. *The Journal of Immunology*, *160*(10), 5088–5097.

[40] Lindorfer, M. A., Nardin, A., Foley, P. L., Solga, M. D., Bankovich, A. J., Martin, E. N., Henderson, A. L., Price, C. W., Gyimesi, E., Wozencraft, C. P., Goldberg, J. B., Sutherland, W. M., & Taylor, R. P. (2001). Targeting of Pseudomonas aeruginosa in the Bloodstream with Bispecific Monoclonal Antibodies. *The Journal of Immunology*, *167*(4), 2240–2249. https://doi.org/10.4049/jimmunol.167.4.2240

[41] Gyimesi, E., Bankovich, A. J., Schuman, T. A., Goldberg, J. B., Lindorfer, M. A., & Taylor, R. P. (2004). Staphylococcus aureus bound to complement receptor 1 on human erythrocytes by bispecific monoclonal antibodies is phagocytosed by acceptor macrophages. *Immunology Letters*, *95*(2), 185–192. https://doi.org/10.1016/j.imlet.2004.07.007

[42] Kobayashi, T., Takauchi, A., Spriel, A. B. van, Vilé, H. A., Hayakawa, M., Shibata, Y., Abiko, Y., Winkel, J. G. J. van de, & Yoshie, H. (2004). Targeting of Porphyromonas gingivalis with a bispecific antibody directed to FcαRI (CD89) improves in vitro clearance by gingival crevicular neutrophils. *Vaccine*, *23*(5), 585–594. https://doi.org/10.1016/j.vaccine.2004.07.015

[43] Tacken, P. J., Hartshorn, K. L., White, M. R., Kooten, C. van, Winkel, J. G. J. van de, Reid, K. B. M., & Batenburg, J. J. (2004). Effective Targeting of Pathogens to Neutrophils via Chimeric Surfactant Protein D/Anti-CD89 Protein. *The Journal of Immunology*, *172*(8), 4934–4940. https://doi.org/10.4049/jimmunol.172.8.4934

[44] Bruno, J. G., Carrillo, M. P., & Crowell, R. (2009). Preliminary development of DNA aptamer-Fc conjugate opsonins. *Journal of Biomedical Materials Research Part A*, *90A*(4), 1152–1161. https://doi.org/10.1002/jbm.a.32182

[45] Katzenmeyer, K. N., & Bryers, J. D. (2011). Multivalent artificial opsonin for the recognition and phagocytosis of Gram-positive bacteria by human phagocytes. *Biomaterials*, *32*(16), 4042–4051. https://doi.org/10.1016/j.biomaterials.2011.02.007

[46] Springer International Publishing. (2017). Anti-antimicrobial Approaches to Device-Based Infections. In *Antimicrobial Coatings and Modifications on Medical Devices* (pp. 143–170).

[47] Katzenmeyer, K. N., Szott, L. M., & Bryers, J. D. (2017). Artificial opsonin enhances bacterial phagocytosis, oxidative burst and chemokine production by human neutrophils. *Pathogens and Disease*, *75*(6). https://doi.org/10.1093/femspd/ftx075

[48] FlowJo, LLC. (2020). Comparison Algorithms. https://docs.flowjo.com/flowjo/experiment-based-platforms/population-comparison/plat-comparison-univariate/

[49] FlowJo, LLC. (2017). Population Comparison - Overview. http://v9docs.flowjo.com/html/comparison.html

[50] Taciak, B., Białasek, M., Braniewska, A., Sas, Z., Sawicka, P., Kiraga, Ł., Rygiel, T., & Król, M. (2018). Evaluation of phenotypic and functional stability of RAW 264.7 cell line through serial passages. *PloS one*, *13*(6), e0198943. https://doi.org/10.1371/journal.pone.0198943

[51] Abcam. (n.d.). Counting cells using a hemocytometer. https://www.abcam.com/protocols/counting-cells-using-a-haemocytometer

[52] Lowe, D. M., Bangani, N., Mehta, M. R., Lang, D. M., Rossi, A. G., Wilkinson, K. A., Wilkinson, R. J., & Martineau, A. R. (2013). A novel assay of antimycobacterial activity and phagocytosis by human neutrophils. *Tuberculosis*, *93*(2), 167–178. https://doi.org/10.1016/j.tube.2012.11.014

[53] Chaka, W., Scharringa, J., Verheul, A. F., Verhoef, J., Van Strijp, A. G., & Hoepelman, I. M. (1995). Quantitative analysis of phagocytosis and killing of Cryptococcus neoformans by human peripheral blood mononuclear cells by flow cytometry. *Clinical and Diagnostic Laboratory Immunology*, *2*(6), 753–759. https://doi.org/10.1128/CDLI.2.6.753-759.1995

[54] Ninković, J., & Roy, S. (2014). High throughput fluorometric technique for assessment of macrophage phagocytosis and actin polymerization. *Journal of visualized experiments: JoVE*, (93), e52195. https://doi.org/10.3791/52195

[55] Triantafilou, K., Triantafilou, M., & Fernandez, N. (2000). Lipopolysaccharide (LPS) labeled with Alexa 488 hydrazide as a novel probe for LPS binding studies. *Cytometry*, *41*(4), 316–320. https://doi.org/10.1002/1097-0320(20001201)41:4<316::AID-CYTO10>3.0.CO;2-Z

[56] Sigma-Aldrich, Inc. (2008, August). Fluorescein Isothiocyanate. https://www.sigmaaldrich.com/content/dam/sigma-aldrich/docs/Sigma/Product_Information_Sheet/f7250pis.pdf

[57] Ribes, S., Ebert, S., Regen, T., Agarwal, A., Tauber, S. C., Czesnik, D., Spreer, A., Bunkowski, S., Eiffert, H., Hanisch, U. K., Hammerschmidt, S., & Nau, R. (2010). Toll-like receptor stimulation enhances phagocytosis and intracellular killing of nonencapsulated and encapsulated Streptococcus pneumoniae by murine microglia. *Infection and immunity*, *78*(2), 865–871. https://doi.org/10.1128/IAI.01110-09

[58] Tsaousis, K. T., Kopsachilis, N., Tsinopoulos, I. T., Dimitrakos, S. A., Kruse, F. E., & Welge-Luessen, U. (2013). Time-dependent morphological alterations and viability of cultured human trabecular cells after exposure to Trypan blue. *Clinical & Experimental Ophthalmology*, *41*(5), 484–490. https://doi.org/10.1111/ceo.12018

[59] Chan, L. L.-Y., Rice, W. L., & Qiu, J. (2020). Observation and quantification of the morphological effect of trypan blue rupturing dead or dying cells. *PLOS ONE*, *15*(1), e0227950. https://doi.org/10.1371/journal.pone.0227950

[60] Bicker, H., Höflich, C., Wolk, K., Vogt, K., Volk, H.-D., & Sabat, R. (2008). A Simple Assay to Measure Phagocytosis of Live Bacteria. *Clinical Chemistry*, *54*(5), 911–915. https://doi.org/10.1373/clinchem.2007.101337

[61] Gille, C., Spring, B., Tewes, L., Poets, C. F., & Orlikowsky, T. (2006). A new method to quantify phagocytosis and intracellular degradation using green fluorescent protein-labeled

Escherichia coli: Comparison of cord blood macrophages and peripheral blood macrophages of healthy adults. *Cytometry Part A*, *69A*(3), 152–154. https://doi.org/10.1002/cyto.a.20222